



저작자표시-비영리-변경금지 2.0 대한민국

이용자는 아래의 조건을 따르는 경우에 한하여 자유롭게

- 이 저작물을 복제, 배포, 전송, 전시, 공연 및 방송할 수 있습니다.

다음과 같은 조건을 따라야 합니다:



저작자표시. 귀하는 원저작자를 표시하여야 합니다.



비영리. 귀하는 이 저작물을 영리 목적으로 이용할 수 없습니다.



변경금지. 귀하는 이 저작물을 개작, 변형 또는 가공할 수 없습니다.

- 귀하는, 이 저작물의 재이용이나 배포의 경우, 이 저작물에 적용된 이용허락조건을 명확하게 나타내어야 합니다.
- 저작권자로부터 별도의 허가를 받으면 이러한 조건들은 적용되지 않습니다.

저작권법에 따른 이용자의 권리는 위의 내용에 의하여 영향을 받지 않습니다.

이것은 [이용허락규약\(Legal Code\)](#)을 이해하기 쉽게 요약한 것입니다.

[Disclaimer](#)

치의과학박사 학위논문

Regulation of macrophage polarization by
surface-grafted phosphatidylserine liposomes

표면 개질된 포스파티딜세린 리포솜에 의한
대식세포 분극 조절

2021년 8월

서울대학교 대학원
치의과학과 치과생체재료과학 전공
김용준

Regulation of macrophage polarization by
surface-grafted phosphatidylserine liposomes

표면 개질된 포스파티딜세린 리포솜에 의한
대식세포 분극 조절

지도교수 양형철

이 논문을 치의과학 박사 학위논문으로 제출함
2021년 5월

서울대학교 대학원
치의과학과 치과생체재료과학 전공
김용준

김용준의 치의과학 박사 학위논문을 인준함
2021년 7월

위원장 _____
부위원장 _____
위원 _____
위원 _____
위원 _____

Abstract

Regulation of macrophage polarization by surface-grafted
phosphatidylserine liposomes

Kim Yongjoon

Department of Dental Biomaterials Science,

School of Dentistry, Seoul National University

(Directed by Professor Yang Hyeong-Cheol, PhD.)

Macrophages play a key role during inflammatory response to foreign body materials. The cytokines secreted from M1/M2 phenotypes of macrophages participate differently to wound healing and bone formation. In previous studies, phosphatidylserine liposomes (PSL) were used to mimic apoptotic cells to enhance anti-inflammatory response of the macrophages. The purpose of this study was to surface-graft the PSLs and modulate the polarization of the macrophages during inflammatory response to foreign body materials.

First, PSLs were surface-grafted with arginine-glycine-aspartate (RGD). RGD was for mimicking the RGD-motif of milk fat globule-epidermal growth factor-factor 8 (MFG-E8). The RGD-motif binds to $\alpha v\beta 3/\alpha v\beta 5$ -integrins on macrophages to induce phagocytosis and promote anti-inflammatory activities of the macrophages. In in vitro assays, mRNA level of arginase-1 (arg-1), FIZZ1 and YM-1

significantly increased in 3 % (mole % of RGD in PSLs) RGD-PSLs compare to 0 % RGD-PSLs in bone marrow derived macrophages (BMDM). Also protein levels of arg-1 and CCL17 were also significantly higher in 3 % RGD-PSLs compare to 0 % RGD-PSLs. Furthermore, LPS-induced M1 macrophages were suppressed with 3 % RGD-PSLs; mRNA levels of IL-1 β , IL-6 and TNF- α were significantly suppressed compared to 0 % and 1 % RGD-PSLs. Similar results were shown in iNOS and TNF- α ELISA assays. FACs and immunofluorescence analysis also showed that 3 % RGD-PSLs enhanced M2 polarization of macrophages and suppressed LPS-induced M1 polarization. BMDM treated with N-(6-tetramethylrhodaminethiocarbamoyl)-1,2-dihexadecanoyl-sn-glycero-3-phosphatidyl ethanol-amine (TRITC-DHPE) labeled liposomes showed highest level of liposome-engulfment in 3 % RGD-PSLs.

In in vivo experiment, RGD-PSLs entrapped alginate-gelatin matrix were embedded in polyvinyl alcohol (PVA) and subcutaneously implanted into Sprague Dawley (SD) rats. After 1 week, tissue ingrowth into the PVA scaffolds were measured and polarization of macrophages were analyzed with immunohistochemical staining. After 4 weeks, thickness of fibrous capsule around the PVA were measured with Masson's trichrome staining. The results showed that after 1 week, carrageenan induced M1 macrophages were suppressed by 0 % and 3 % RGD-PSLs compared to carrageenan group, but there were no significant differences in number of M2 macrophages within the experimental groups. However, 3 % RGD-PSLs showed highest level of tissue ingrowth after 1 week, and significant decrease in fibrous capsule thickness after 4 weeks. These results imply that 3 % RGD-PSLs enhanced phagocytosis and promoted anti-inflammatory activities of macrophages, while

suppressing M1 macrophage polarization. Also that fibrous capsules are more associated with pro-inflammatory macrophages than anti-inflammatory macrophages.

Another grafting used was polyethylene-glycol (PEG). PEG-grafted PSLs (PEG-PSL) suppressed TGF- β secretion and multinucleated giant cell (MGC) formations in IL-4-treated RAW 264.7. While, PSLs-only did not show inhibitory effect in TGF- β secretion but suppressed MGC formation. In in vivo assays, PEG-PSLs-entrapped alginate-gelatin matrix were coated on mixed cellulose ester (MCE) membranes and were subcutaneously implanted into the dorsal of SD rats. After four weeks of implantation, thickness of fibrous encapsulation around the MCE membranes were analyzed. PEG-PSLs significantly reduced the thickness of fibrous capsule, while PSLs did not show any effect. Because TGF- β is an important factor mediating in fibrous capsule, the results suggest that reduction of fibrous capsule formation by PEG-PSLs via suppression of TGF- β secretion from macrophages.

The results from in vitro and in vivo experiments with RGD and PEG surface-grafted PSLs differently effected the polarization of macrophages. We have demonstrated increase in anti-inflammatory effect of PSLs with 3 % RGD surface-grafting and suppression of TGF- β and fibrous capsule with PEG-PSLs. These results show potential use of surface-grafting of PSLs to modulate macrophage polarizations and clinical uses such as wound healing and bone formation.

Keyword : Macrophage, Polarization, Phosphatidylserine, Liposome, Arginine-glycine-aspartate, Polyethylene Glycol.

Student Number : 2016-39051

Table of Contents

Abstract.....	i
List of Contents.....	iv
Chapter 1. Introduction.....	1
1.1 Macrophages in Inflammatory Responses	
1.1.1 Macrophage Polarization during Inflammatory Response	
1.1.2 Enhancing Polarization of M2 Macrophages	
1.1.3 Phosphatidylserine on Apoptotic Cells	
1.1.4 RDG-motif of Milk Fat Globule-E8	
1.2 1.2 Macrophages in Foreign Body Reaction	
1.2.1 Fibrous Capsule Formation	
1.2.2 Reducing Fibrous Capsule by Regulating TGF- β	
1.2.3 Polyethylene-Glycol	
Chapter 2. Materials and Methods.....	10
2.1 Effect of RGD-PSLs on Macrophage Polarization	
2.1.1 Liposome Preparation	
2.1.2 Bone Marrow Isolation and Induction to BMDM	
2.1.3 RT-PCR, ELISA and Nitric Oxide Assay	
2.1.4 Flow Cytometry and Immunofluorescence	
2.1.5 Liposome Uptake by BMDM	
2.1.6 Alginate-Gelatin Matrix Containing PVA	
2.1.7 Animal Experiment	
2.2 Effect of PEG-PSLs on Fibrous Capsule	
2.2.1 Liposome Preparation	
2.2.2 RAW 264.7 Cell Culture	

2.2.3 RT-PCR and ELISA of TGF- β	
2.2.4 Multinucleated Giant Cell formation	
2.2.5 Cell Attachment Assay	
2.2.6 MCE Membrane Coated with Alginate-Gelatin Matrix	
2.2.7 Fluorescence-labeled Liposomes in Alginate-Gelatin Matrix	
2.2.8. Subcutaneous implantation of MCE membrane	
Chapter 3. Results	21
3.1 Effect of RGD-PSLs on Macrophage Polarization	
3.1.1 M1 and M2 Macrophage Polarization	
3.1.2 Flow Cytometry and Immunofluorescence	
3.1.3 Liposome Uptake by BMDM	
3.1.4 Tissue Ingrowth and Fibrous Encapsulation	
3.1.5 Polarization of Macrophages Recruited to Surrounding Tissues	
3.2 Effect of PEG-PSLs Fibrous Capsule	
3.2.2 The Size of Liposomes and the Spatial Disposition of PSLs in Alginate-Gelatin Mixture	
3.2.3 Effect of PEG-PSLs on TGF- β expression	
3.2.4. Effect of PEG-PSLs on MGC formation	
3.2.5. Macrophage attachment to alginate-gelatin matrix	
3.2.6. Histological observation and fibrous encapsulation analysis	
Chapter 3. Discussion	44
Chapter 4. Conclusion	49
References	50
Abstract in Korean	55

Chapter 1. Introduction

1.1 Macrophages in Inflammatory Responses

1.1.1 Macrophage Polarization during Inflammatory Responses

Macrophages play a critical role during the inflammatory responses. Depending on the polarization of the macrophages, different chemokine and cytokines are secreted, participating in host defense and wound healing including tissue repair and tissue regeneration (Watanabe et al., 2019). The macrophages are originated from the bone marrow which are differentiated into monocytes at the wound site (Wynn & Vannella, 2016; Ziegler-Heitbrock et al., 2010). The differentiated macrophages are polarized into two different phenotypes: classically activated M1 and alternatively activated M2 (Fig. 1). In presence of tumor necrosis factor (TNF) or lipopolysaccharide (LPS), the macrophages express toll-like receptors (TLR) inducing transcription of TNF and M1 macrophage polarizations (Cho et al., 2014; Sheikh et al., 2015). The M1 macrophages play a key role in host defending through secreting pro-inflammatory cytokines such as IL-1 β , IL-6 and TNF- α (Kim et al., 2016). In presence of IL-4 secreted from mast cells and basophil, macrophages are polarized to M2 phenotypes, promoting wound healing and tissue repair (Sheikh et al., 2015). The M2 macrophages secrete very low level of pro-inflammatory cytokines with high levels of anti-inflammatory cytokines such as IL-10 and TGF- β (Mosser & Edwards, 2008; Wynn & Vannella, 2016; Zhang et al., 2016). Furthermore, the anti-inflammatory cytokines secreted from M2 macrophages induce activation of mesenchymal stem cells (MSC) to osteoblastic cells. But on the other hand, M1 macrophages

diminish osteoblastic differentiation of the MSCs (Gong et al., 2016; Gu et al., 2017). For this reason, M2 polarization of macrophages are important in wound healing and bone formation.

1.1.2 Enhancing Polarization of M2 Macrophages

There have been numerous of studies done to enhance M2 macrophage polarization. Previous study by Ren et al. (2008) have demonstrated the effect of PS-exposed apoptotic cells through in vivo experiment. In that study, apoptotic polymorphonuclear neutrophils (PMN) increased survival rate of mice with lipopolysaccharide (LPS)-induced endotoxic shock. Ren et al. (2008) reported that the apoptotic cells were effective in reducing levels of LPS-induced pro-inflammatory cytokines and showed the effect 24 h after LPS induction (Ren et al., 2008). Furthermore, there are studies which demonstrated mimics the anti-inflammatory effect of the apoptotic cells with phosphatidylserine liposomes (PSL). The studies have shown the inhibitory effect of PSLs on nitric oxide (NO) and TNF- α in LPS-treated macrophages while enhancing secretion of TGF- β via extracellular signal-regulated kinases (ERK) signaling pathway (Aramaki et al., 1996; Otusuka et al., 2005). The study by Harel-Adar et al. (2011) have also demonstrated anti-inflammatory effect of the PSLs in macrophages. In the study, PSLs increased secretion of TGF- β and IL-10 and upregulated expression of mannose receptor, while decreasing the pro-inflammatory cytokines. Also in the animal experiment, PSLs showed promotion in angiogenesis and preservation of small scars in acute myocardial infarction rat models (Harel-Adar et al., 2011). Another animal experiment by Ramos et al. (2007), have demonstrated the anti-

inflammatory effect of PSLs in mouse with carrageenan-induced paw edema. The PSLs showed anti-inflammatory effect even after 24 and 48 h of carrageen injection in dose-dependent manner and production of IL-1 β in paws were decreased with the PSLs treatment (Ramos et al., 2007). These results imply that the PSLs are affective in modulation of macrophage polarizations in vivo and have therapeutic potential for inflammatory treatment.

1.1.3 Phosphatidylserine on Apoptotic Cells

Phosphatidylserines (PS) are located in the inner leaflet of lipid bilayer of live cells and move to the outer leaflet during apoptosis (Callahan et al., 2003). The exposed PS express “find me” and “eat me” signals and promote recruitment of macrophages (Naeini et al., 2020). The recruited macrophages clear the apoptotic cells by phagocytosis through PS-PS receptor binding (Fadok et al., 2000). The clearance of the apoptotic cells through phagocytosis is important for reducing the pro-inflammatory cytokines and enhance anti-inflammatory cytokines (Borisenko et al., 2003; Kusunoki et al., 2012).

PS on apoptotic cells bind with PS-receptors on macrophages through direct and indirect bindings. For direct bindings, PS apoptotic cells bind to PS-receptors on macrophages inducing phagocytosis. The PS-binding receptors are such as T-cell membrane protein (TIM) family including brain angiogenesis inhibitor 1 (BAI 1), TIM family and stabilin (Fig. 2. A) (Kourtzelis et al., 2020). The indirect bindings require molecular bridges between the PS and receptors. The bridging molecules include growth arrest-specific gene 6 (GAS6) and

milk fat globule-E8 (MFG-E8). GAS6 binds to TAM receptors such as MerTK on macrophages through carboxyl terminal domains and PS with their amino terminal domains (Fig. 2. B) (Myers et al., 2019; Naeini et al., 2020). MFG-E8 promotes binding to $\alpha\text{v}\beta\text{3}/\alpha\text{v}\beta\text{5}$ -integrins on macrophages and PS on apoptotic cell (Fig. 2. B) (Kourtzelis et al., 2020).

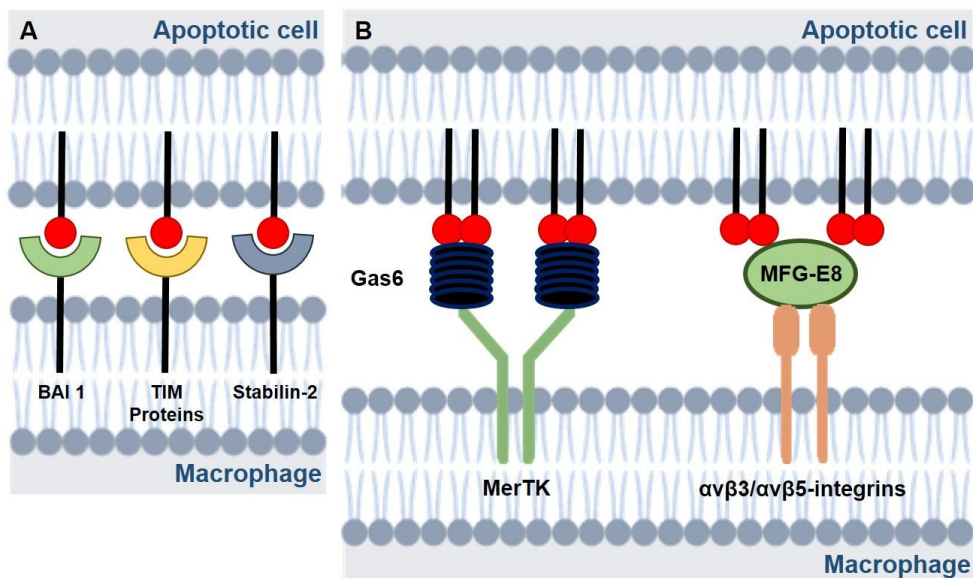


Figure 2. Direct and indirect binding of PS on apoptotic cells and receptors on macrophages. A) Direct binding of PS and PS receptors. PS receptors on macrophages include brain angiogenesis inhibitor 1 (BAI 1), TIM family (ie. TIM-1 and TIM-4) and stabilin. B) Molecular bridges for indirect bindings: Gas6 and MFG-E8. GAS6 binds to MerTK of macrophages and amino terminal domains bind to PS. MFG-E8 binds to $\alpha\text{v}\beta\text{3}/\alpha\text{v}\beta\text{5}$ -integrins of macrophages and PS on apoptotic cell.

1.1.4 RDG-motif of Milk Fat Globule-E8

MFG-E8 is a glycoprotein secreted from various cells, which induces engulfment by binding to PS on apoptotic cells and $\alpha\text{v}\beta\text{3}/\alpha\text{v}\beta\text{5}$ -

integrins of macrophages (Kusunoki et al., 2012; Yamada et al., 2016). The structure of MFG-E8 possesses two discoidin-like domains resembling blood coagulation factor V/V111 at the C-terminal and two epidermal growth factor (EGF) repeated at the N-terminal end (Kusunoki et al., 2012). An arginine-glycine-aspartate (RGD) motif contained in the second EGF repeat, binds with the $\alpha v\beta 3/\alpha v\beta 5$ -integrins on macrophages and discoidin-like domains bind to the PS on apoptotic cells (Fig. 3) (Das et al., 2016). Binding of MFG-E8 and $\alpha v\beta 3/\alpha v\beta 5$ -integrins activates Rac1, resulting cytoskeletal remodeling in macrophages and promote phagocytosis of the liposomes (Fuller & Van Eldik, 2008). Brissette et al. (2012) have reported that MFG-E8 released from apoptosis of endothelial cells promote macrophages to anti-inflammatory state through phosphorylation of signal transducer and activator of transcription-2 (STAT-3) (Brissette et al., 2012). In another study by Das et al., demonstrated that MFG-E8-knockout (MFG-E8^{-/-}) C57BL/6 mice showed impaired inflammatory response, poor angiogenesis and wound closure. Also transplantation of MFG-E8^{-/-} bone marrow to wild-type (MFG-E8^{+/+}) mice resulted in impaired wound closure and compromised vascularization, while MFG-E8^{-/-} mice which received MFG-E8^{+/+} bone marrow showed improve in wound closure and vascularization (Das et al., 2016). Thus, it can be hypothesis that, by mimicking MFG-E8 with RGD on PSLs will promote phagocytosis and induce polarization of M2 macrophages and enhance anti-inflammatory effect of PSLs.

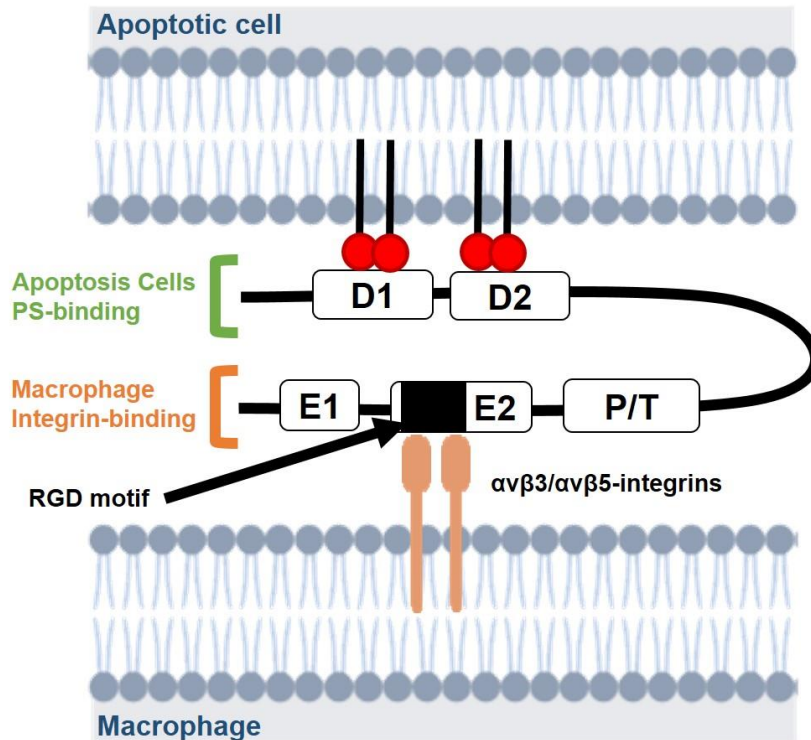


Figure 3. MFG-E8 is a glycoprotein and a bridge molecule which binds between PS on apoptotic cells and $\alpha\beta3/\alpha\beta5$ -integrins on macrophages. The MFG-E8 possess two discoidin-like domains resembling blood coagulation factor V/V111 at the C-terminal and two epidermal growth factor (EGF) repeated at the N-terminal end. An arginine-glycine-aspartate (RGD) motif contained in the second EGF repeat, binds with the $\alpha\beta3/\alpha\beta5$ -integrins on macrophages and discoidin-like domains bind to the PS on apoptotic cells.

1.2 Macrophages in Foreign Body Reaction

1.2.1 Fibrous Capsule Formation

The implanted foreign body materials induce inflammatory responses from the host immune system trying exterminate the materials (Kim et al., 2016). However, this can result local discomfort or pain to the patients and limit the function of the implant by fibrous capsule formation on the surfaces (Mosser & Edwards, 2008). For example,

medical devices such as biosensor senses analytes such as glucose, diffused to sensing membranes, but development of fibrous capsule layer on the surface of the devices can disturb the diffusion of analytes to the sensors (Kenneth Ward, 2008).

Prolonged existence of foreign body materials and secretion of IL-4 and IL-13 from mast cells induce expression of mannose receptors on macrophages, which promote fusion to foreign body multinucleated giant cells (FBGC) (Anderson et al., 2008; Brodbeck & Anderson, 2009). However, the FBGCs are another source of TGF- β (Kenneth Ward, 2008). One of the roles of the TGF- β is to recruit tissue repair cells such as fibroblasts and differentiate them into myofibroblasts. Differentiated myofibroblasts synthesize extra cellular matrix (ECM) resulting fibrous capsule on the surface of implanted devices (Hinz, 2007; Kim et al., 2016). For this reason, controlled secretion of TGF- β is important for facilitated reconstruction of tissue (Kim et al., 2016).

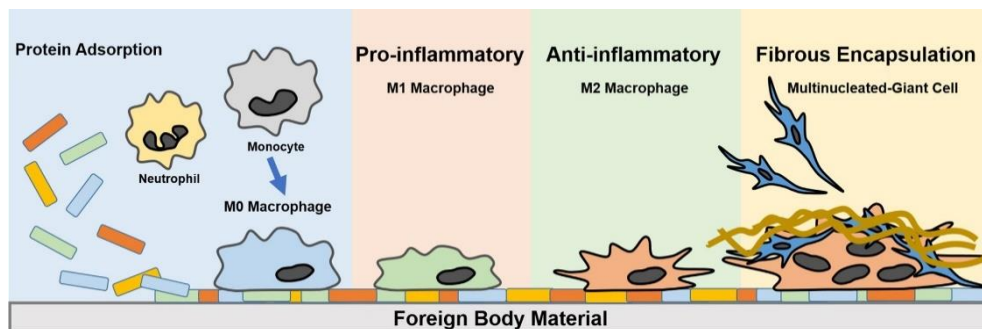


Figure 1. Polarization of bone marrow-derived macrophages: Non-specific proteins absorbed to the surface of foreign body materials, and the immune cells such as neutrophils and monocyte-derived macrophages are recruited. The macrophages polarize into pro-inflammatory M1 macrophages, and anti-inflammatory M2 macrophages. In presence of IL-4 from mast cells and basophils, the macrophage are fused to foreign body multinucleated giant cells (FBGC). The chemokines and

cytokines secreted from the M2 macrophages and FBGCs recruit tissue repair cells such as fibroblasts and differentiate to myofibroblasts which synthesize collagens resulting fibrous capsule on the surfaces of foreign body materials.

1.2.2 Reducing Fibrous Capsule by Regulating TGF- β

Previously, different strategies have been employed to reduced formation of fibrous capsule on the surface of subcutaneous implants. Sevilla et al . (2018) have showed potential use of TGF- β inhibitory peptides for reducing fibrosis on titanium surfaces (Sevilla et al., 2018). In previous study by Park (2015), have used TGF- β inhibitor, tranilat to coat the surface of silicone implant and suppressed the formation of fibrosis on the surfaces (Park et al., 2015). Also in another study, SB-525 334, which is also a TGF- β inhibitor, loaded on electrospun scaffolds prevented fibrotic scars (Wang et al., 2017B).

1.2.3 Polyethylene-glycol

Polyethylene-glycol (PEG) grafting is used to extend half-life of liposomes by avoiding the body clearance machinery (Klibanov et al., 1990). PEG-grafted PSLs (PEG-PSLs) showed delayed clearance in mice circulation, compared to ungrafted PSLs (Levchenko et al., 2002). The stealth effect of PEG grafting on PSLs can be attributed to the steric hinderance provided by the PEG. Because the PS-PS receptor interaction is important in macrophage immunomodulation, PEG-grafting is expected to have an effect on activities of macrophages. In fact, in our previous study, we have demonstrated different pattern of cytokine secretion with the PEG-PSLs compare

to the PSLs-treated group (Quan et al., 2017). Our results showed that PEG-grafting decreased LPS-induced TNF- α and suppressed secretion of TGF- β compared to the PSLs only. Because TGF- β play a key role in recruiting fibroblasts and differentiate to myofibroblasts to synthesize fibrous capsule, it can be hypothesized that by using PEG-PSLs foreign body induced fibrous capsule can be reduced.

Chapter 2. Materials and methods

2.1 Assessment of RGD-PSLs on Macrophage Polarization

2.1.1 Liposome Preparation

All experimental reagents were purchased from Sigma-Aldrich Co. (Saint Louis, MO, USA), unless otherwise specified. PSLs were prepared following an extrusion method. Briefly, PS, phosphatidylcholine (PC), and cholesterol (CH) were dissolved in chloroform/methanol (9:1 v/v) in a molar ratio of 2:1:1 (PS:PC:CH). The solvent was evaporated by N₂ gas, and the residual solvent was removed using a vacuum chamber for 2 h. The remaining lipid film was hydrated in phosphate-buffered saline for 1 h, followed by vortexing for 30 s. The liposomes were sized by using a mini-extruder (Avanti Polar Lipids, Alabster, AL, USA) with a polycarbonate filter of 400 nm and 100 nm pore size. The final concentration of PS in the liposome suspension was 1.25 mM. For the preparation of RGD-PSLs, 1 %, 3 % and 5 % (mol %) RGD (DSPE-RGD, Avanti Polar, Alabaster, AL, USA) was added prior to the evaporation step. The size of the liposomes was measured by nanoparticle tracking analyzer (NanoSight, Malvern Panalytical, Malvern, UK).

2.1.2 Bone Marrow Isolation and Induction to BMDM

All experiments and procedures with animals were approved by the Institutional Animal Care and Use Committee in Seoul National University. Throughout the experiment, bone marrow-derived macrophages (BMDM) were collected from five-week-old ICR male

mice (OrientBio Inc., Seongnam, Korea) and all the procedures were done under aseptic conditions. Briefly, for bone marrow isolation, the mice were sacrificed humanely and femur bones were extracted by removing surrounding muscles. The joints were cut and bone marrow was flushed out from the end of the bone using a syringe filled with PBS. The collected bone marrow was centrifuged at 1500 rpm for 5 min at room temperature. The supernatant was discarded and the bone marrow pellet was resuspended with R10 media (RPMI 1640, supplemented with 10 % FBS, 1 % antibiotics and 5 mL 1M HEPES, Gibco BRL, Grand Island, NY) containing 5 % DMSO for storage. 1×10^6 bone marrow cells were cultured in a well of a 12 well plate with R10 media containing macrophage colony-stimulating factor (M-CSF, 20 ng mL⁻¹, Sigma Aldrich, Saint Louis, MO) for 24 h. Next day, 1 mL of fresh R10 media was added to each well. On day 2 1 mL of supernatant was removed from each well, and supplemented with 1 mL of R10 media containing M-CSF for another 24 h. On day 4, the supernatant was replaced with 1 mL of fresh R10 media for experiment.

Table 1. Sequences of primers used in RT-PCR.

	Primer Sequence
IL-1 β	forward 5'-TGGAGAGTGTGGATCCCAAG-3'
	reverse 5'-GGTGCTGATGTACCAGTTGG-3'
IL-6	forward 5'-ATAGTCCTTCTACCCCAATTTCC-3'
	reverse 5'-GATGAATTGGATGGTCTTGGTCC-3'
TNF- α	forward 5'-GGCAGGTCTACTTTGGAGTCATTGC-3'
	reverse 5'-ACATTTCGAGCCAGTGAATTCGG-3'
Arg-1	forward 5'-CTCCAAGCCAAAGTCCTTAGAG-3'
	reverse 5'-AGGAGCTGTCATTAGGGACATC-3'
FIZZ1	forward 5'-GGTCCCAGTGCATATGGATGAGACCATAGA-3'
	reverse 5'-CACCTCTCACTCGAGGGACAGTTGGCAGC-3'
YM-1	forward 5'-CAGGGTAATGAGTGGGTTGG-3'
	reverse 5'-CACGGCACCTCCTAAATTGT-3'
GAPDH	forward 5'-TGTGTCCGTCGTGGATCTGA-3'
	reverse 5'-CCTGCTTCACCACCTTCTTGAT-3'

2.1.3 RT-PCR, ELISA and Nitric Oxide Assay

The effect of RGD-PSLs on expression of pro-inflammatory and anti-inflammatory related markers were analyzed by RT-PCR. To assess the pro-inflammatory cytokines, BMDM were co-treated with RGD-PSLs and lipopolysaccharide (LPS, 50 ng mL⁻¹, Escherichia coli, serotype O55:B5) for 12 h. To assess the anti-inflammatory cytokines, BMDM were treated with RGD-PSLs only for 12 h. After 12 h, total RNA was isolated from the cells and cDNA was synthesized for RT-PCR following the protocols previously described. The sequences of the primers used are arranged in Table 1.

To assess the secretion of TNF- α and CCL17 in the culture media, supernatants were subsequently collected after 12 h of cell treatment and analyzed using ELISA kits (Quantikine HS, R&D Systems, Inc., Minneapolis, MN) according to the manufacturer's instructions. To

assess arginase-1 (arg-1), the cells were lysed after 12 h treatment using Pro-PrepTM (iNtRON Biotechnology, Sungnam, Korea) and analyzed using an ELISA kit (Abbexa LLC, Houston, USA) following manufacturers' instructions. For nitric oxide assay (Abcam, Cambridge, UK), supernatant was collected after cell treatment and performed following the manufacturer's instructions.

2.1.4 Flow Cytometry and Immunofluorescence

After 12 h of RGD-PSL treatment with/without LPS, the activation state of BMDM were confirmed using flow cytometry and immunofluorescence staining. CD68 was used for pan-macrophage marker and CD86 and CD206 were used for the M1 and M2 markers, respectively. For flow cytometry, BMDM were stained with Alexa flour®-conjugated antibodies (BioLegend, San Diego, CA) for 15 min at 4°C and analyzed with a flow cytometer (FACS-Calibur; Becton-Dickinson, San Jose, CA). For immunofluorescence staining, BMDM were stained with the antibodies for 2 h in room temperature after fixing with 4 % paraformaldehyde, permeabilizing with 0.5 % Triton X-100 and blocking with 3 % BSA for 15 min, 5 min and 1 h in room temperature, respectively. The immunofluorescence images were obtained with a laser scanning confocal microscope (Carl Zeiss, Oberkochen, Germany).

2.1.5 Liposome Uptake by BMDM

RGD-PSL uptake by BMDM were analyzed with a laser scanning confocal microscope (Carl Zeiss, Oberkochen, Germany). RGD-PSL were labeled with 0.5 mol % N-(teramethylrhodamine-6-thiocarbamoyl)-1, 2-dihexadecanoyl-sn-glycero-3-phosphoethanolamine (TRITC-DHPE, Biotium Inc., Hayward, CA) at

the beginning of phospholipid mixing stage. After 3 h of TRITC-DHPE-labeled RGD-PSL treatment, mounting solution with 4', 6-diamidino-2-phenylindole (DAPI, Santa Cruz Biotechnology, Dallas, TX) was added. The uptake images of RGD-PSL by BMDM were obtained with a laser scanning confocal microscope (Carl Zeiss, Oberkochen, Germany).

2.1.6 Alginate-Gelatin Matrix Containing PVA

All procedures for sample preparation were performed under sterile conditions. An aqueous solution containing 2 % (w/v) sodium alginate and 5 % gelatin (porcine skin Type A) was autoclaved at 121 °C for 15 min, cooled down to room temperature. For experimental groups, 1 % (w/v) carrageenan was added prior to autoclave stage. Prepared aqueous solution was mixed with liposome suspension in a 1:1 (v/v) ratio. The mixtures were added to sterilized PVA (Polyvinyl alcohol, Sam Kwang, Daegu, Korea), and crosslinked with 100 mM CaCl₂ for 30 min. The size of PVA for implantation in animal experiments were 5 x 5 mm² with 1+/- 0.1 mm thickness.

2.1.7 Animal Experiment

Five-week-old Sprague Dawley male rats (OrientBio Inc., Seongnam, Korea) were divided into six groups (namely, negative control, positive control, 0 % RGD-PSL, 1 % RGD-PSL, 3 % RGD-PSL, 5 % RGD-PSL) (n = 6). The rats were anesthetized by intraperitoneal injections with ketamine (Yuhan Co., Kunpo, Korea) and xylazine (Rompun, Bayer HealthCare, Leverkusen, Germany) in a 2:1 (v/v) ratio. Two subcutaneous pockets were made on the dorsal of each rat, and PVA containing liposomes were placed into the pocket and sutured. After one week and four weeks, the rats were sacrificed and

PVA with surrounding tissue were harvested. The harvested tissues were sectioned and stained with H&E and Masson's trichrome staining. The images were obtained by a light microscope (DM5000B, Leica, Wetzlar, Germany) equipped with a digital camera (DFC550, Leica). Using a software (ImageJ, National Institute of Health, USA), total area of PVA and tissue ingrowth areas were measured and average percentage of tissue ingrowth for each sample groups were calculated.

2.2 Assessment of PEG-PSLs on Fibrous Capsule

2.2.1 Liposome Preparation

PSLs were prepared following the protocol described in 2.1.1 Liposome Preparation, except for PEG-grafting, 1,2distearoyl-sn-glycero-3-phosphoethanolamine-N-[amino(PEG)-2000] (DSPE-PEG-2000) was added prior to the evaporation step. The liposomes were sized with a polycarbonate filter of 400 nm pore size. The finale concentration of PS in the liposome suspension was 1.25 mM and DSPE-PEG-2000 was 25 μ M. For PEG-grafted phosphatidylcholine liposomes (PEG-PCLs) preparation, PC and CH were mixed in a 3:1 molar ratio. The size of the liposomes was measured by nanoparticle tracking analyzer (NanoSight, Malvern Panalytical, Malvern, UK).

2.2.2 RAW 264.7 Cell Culture

RAW 264.7 cell line was obtained from RIKEN Cell Bank (Tsukuba, Japan) and maintained in a Macrophage Serum-Free Meidum (M-SFM, Gibco-BRL, Grand Island, NY, USA) supplemented with antibiotics (100 U mL⁻¹ penicillin-G and 100 mg mL⁻¹ streptomycin) at 37 °C in a humidified atmosphere (5 % CO₂ / 95 % air).

Table 2. Sequences of primers used in RT-PCR.

	Primer Sequence
TGF- β	forward 5'-TGGAGCAACATGTGGAAGTC-3'
	reverse 5'-TGCCGTACAACCTCCAGTGAC-3'
GAPDH	forward 5'-TGTGTCCGTCGTGGATCTGA-3'
	reverse 5'-CCTGCTTCACCACCTTCTTGAT-3'

2.2.3 RT-PCR and ELISA of TGF- β

The effect of PSLs and PEG-PSLs on TGF- β mRNA expression in RAW 264.7 cells was analyzed by RT-PCR. 1×10^5 cells were cultured in a well of a 12-well plate and incubated in M-SFM containing 1 % FBS for 1.5 h, followed by pre-treatment with IL-4 (100 ng mL⁻¹) for 6 h. The IL-4-pre-treated cells were then exposed to liposomes by adding the liposome suspension to each well. The final concentration of total liposomes was 34 μ M (i.e. 17 μ M PS). After treatment for 12 h, total RNA was isolated using an RNA isolation kit (WelPrep Total RNA Isolation Reagent, Welgene Inc., Daegu, Korea). cDNA was synthesized from the total RNA using a cDNA synthesis kit (Power cDNA synthesis kit, iNtRON Biotechnology, Sungnam, Korea). PCR was performed in a 20 μ L reaction mixture containing 10 μ L SYBR Premix Ex Taq (Takar Bio, Otsu, Japan), 0.4 μ L ROX Reference Dye (Takara Bio), cDNA, and primers. The reactions were performed using an ABI PRISM 7300 Sequence Detection Thermal Cycler (Applied Biosystems, Foster City, CA, USA). The sequences of the primers used are arranged in Table 2. The PCR thermocycling conditions were as follows: 95 °C for 30 s followed by 40 cycles of denaturation at 95 °C for 15 s and annealing at 60°C for 30 s. TGF- β mRNA expression levels were

expressed as threshold cycle (CT) values, and the levels were normalized to the reference gene (GAPDH). The secretion of TGF- β cytokine from liposome-treated cells was evaluated by measuring the amount of TGF- β protein in cell cultures. After cells were treated for 12 h in a similar way done for the RT-PCR experiment, an aliquot of culture supernatant was analyzed for TGF- β concentration using an ELISA kit (Quantikine HS, R&D Systems, Inc., Minneapolis, MN) according to the manufacturer's instructions.

Table 3. Time schedule for MGC formation experiments; Co-treatment, Pre-treatment and Pre/Co-treatment.

	Pre-Treatment (6 h)	Co-Treatment (42 h)
Co-Treated	No treatment	Co-Treatment with IL-4 and liposomes
Pre-Treated	Pre-Treatment with liposomes	IL-4 only treatment (without liposomes)
Pre/Co-Treated	Pre-treatment with liposomes	Co-treatment with IL-4 and liposomes

2.2.4 Multinucleated Giant Cell formation

To assess the effect of PEG-PSLs on the formation of multinucleated giant cells (MGC), cell fusion was induced by IL-4 as shown in a previous study. In this study, RAW 264.7 cells were treated in distinct groups over three different time periods as follows: 1) co-treatment, where cells were treated with liposomes for 42 h in the presence of IL-4 (100 ng mL⁻¹); 2) pre-treatment, where cells were pre-treated with liposomes for 6 h, followed by exposure to IL-4 for 42 h without liposomes; and 3) pre/co-treatment, which involved pre-treatment with liposomes for 6 h, followed by co-treatment with

liposomes and IL-4 for 42 h (Table 3.). After treatment, cells were fixed with 3.8% formaldehyde for 3 min and stained with May-Grünwald and Giemsa. Images of the stained cells were acquired using a digital camera equipped microscope. The average number of MGC (more than two nuclei) per each microscopic image was obtained from more than eight different images of each group.

2.2.5 Cell Attachment Assay

To investigate the cell attachment on alginate-gelatin matrices, 1×10^5 of RAW 264.7 cells were cultured in each well of a 12-well plate containing an alginate gelatin matrix for 6 h, and then the matrix was gently washed by PBS, followed by staining with Live/dead cell viability assay kit (Invitrogen, Carlsbad, CA). Calcein-AM-stained live cells were green fluorescent, and ethidium homodimer-1-stained dead cells were red fluorescent. The fluorescence images of live/dead cells were acquired using a digital camera equipped microscope (n = 3 per group). The total numbers of cells per each image frame were counted, and average numbers were calculated for each group.

2.2.6 MCE Membrane Coated with Alginate-Gelatin Matrix

All procedures for sample preparation were performed under sterile conditions. An aqueous solution containing 2 % (w/v) sodium alginate and 5 % gelatin (porcine skin Type A) was autoclaved at 121°C for 15 min, cooled down to room temperature, and mixed with the liposome suspension in a 1:1 (v/v) ratio. The mixture was added to sterilized mixed cellulose ester (MCE) membranes (Advantec Tokyo Kaisha Ltd., Tokyo, Japan), and alginate was crosslinked with 100 mM CaCl_2 for 30 min. The thickness of each alginate-gelatin matrix

was 1 ± 0.1 mm. For implantation in animal experiments, the MCE membranes were cut into 5×5 mm² pieces.

2.2.7 Fluorescence-labeled Liposomes in Alginate-Gelatin Matrix

To confirm homogenous distribution of liposomes in the alginate-gelatin matrix, PSLs were labeled with N-(teramethylrhodamine-6-thiocarbamoyl)-1, 2-dihexadecanoyl-sn-glycero-3-phosphoethanolamine (TRITC-DHPE, Biotium Inc., Hayward, CA) (excitation/ emission = 555/580 nm), and the fluorescent liposomes were observed using a confocal laser scanning microscope (LSM 700, Carl Zeiss, Oberkochen, Germany). TRITC-DHPE was incorporated at the stage of phospholipid mixing (5 mol % of total mixture). A block of the crosslinked alginate-gelatin mixture containing liposomes was mounted on a glass slide using a malinol-based technique (Muto Pure Chemicals, Tokyo, Japan), and 3-D fluorescence images of 35 μ m depth were observed.

2.2.8. Subcutaneous implantation of MCE membrane

Five-week-old Sprague Dawley male rats (OrientBio Inc., Seongnam, Korea), raised under SPF conditions, were randomly divided into four groups (namely, negative control, PSL, PEG-PCL, PEG-PSL) (n = 8 per group), and anesthetized by intraperitoneal injection of ketamine (Yuhan Co., Kunpo, Korea) and xylazine (Rompun, Bayer HealthCare, Leverkusen, German) in a 2:1 (v/v) ratio. Dorsal hairs were shaved, and two subcutaneous pockets were made in the middle of each rat. A coated membrane was placed in each pocket and sutured. After four weeks, the rats were sacrificed humanely, and the MCE membranes along with their surrounding tissues were harvested and

stained by H&E and Masson's trichrome staining. The animal experiments were approved by the Institutional Animal Care and Use Committee in Seoul National University. The images of the stained tissue sections were obtained by a light microscope (DM5000B, Leica, Wetzlar, Germany) equipped with a digital camera (DFC550, Leica). The fibrous capsule thickness was measured from the images of the Masson's trichrome stained sections. The average thickness was obtained by measuring the width of fibrous capsules at five different sites on the coated side of each MCE membrane using ImageJ program (National Institute of Health, Bethesda, MD, USA).

Chapter 3. Result

3.1 Effect of RGD-PSLs on Macrophage Polarization

3.1.1 M1 and M2 Macrophage Polarization

To evaluate the effect of RGD-PSLs on the macrophages polarization, BMDM were treated with the liposomes in two different conditions; liposome co-treatment with LPS for 12 h and liposome only for 12 h. The results showed increase in mRNA expressions of pro-inflammatory cytokines such as IL-1 β , IL-6 and TNF- α with LPS (Fig. 4. A, B and C, respectively) as well as NO and TNF- α protein secretions (Fig. 5 A and B, respectively). With IL-4 co-treatment, mRNA expression of IL-1 β was suppressed, while IL-6 and TNF- α expressed no significant differences compare to LPS only treated group. However, PSLs and 1 % RGD-PSLs suppressed the expressions of LPS-induced IL-1 β and IL-6, and 3 % and 5 % RGD-PSLs groups expressed most suppressed mRNA levels of IL-1 β , IL-6 and TNF- α . The nitric oxide secretion was suppressed with 3 % RGD-PSLs with no significant difference to the negative control group. For TNF- α ELISA, 3 % and 5 % RGD-PSLs showed effective in suppression of the cytokine secretion.

To analyze the anti-inflammatory effect of RGD-PSLs, BMDM were treated with RGD-PSLs only for 12 h. After 12 h, IL-4 increased the mRNA expressions of arg-1, FIZZ1 and YM-1, and also 3 % RGD-PSLs have significantly increased the mRNA expressions of the cytokines among the experimental groups (Fig. 5. E, F and G, respectively). For the protein secretion level of arg-1, 3 % RGD-PSLs showed highest secretion of the protein and for CCL17, the protein secretion was significantly higher than IL-4 group (Fig. 5. C

and D, respectively).

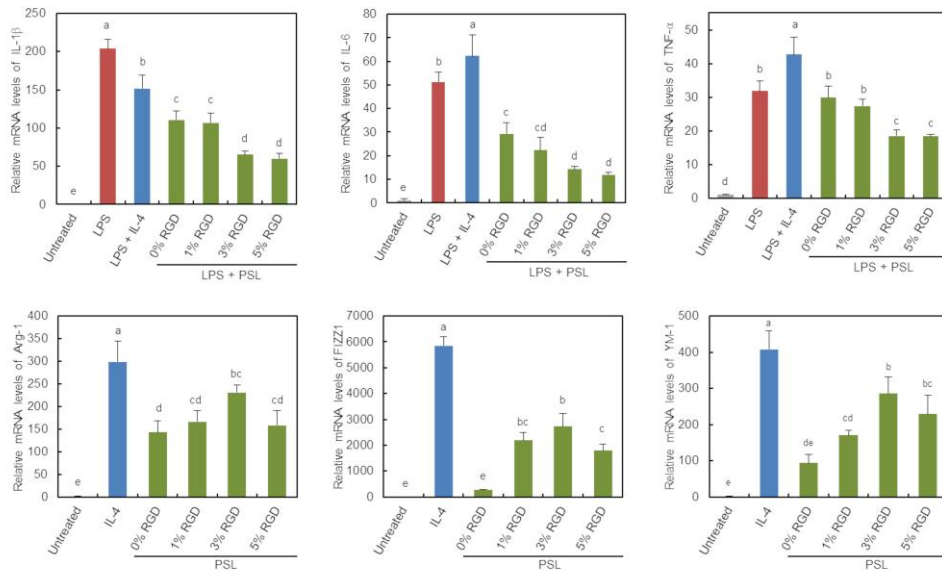


Figure 4. BMDM treated with the liposomes in two different conditions; Liposome co-treatment with LPS for 12 h and liposome only for 12 h. The results showed increase in pro-inflammatory cytokines such as IL-1 β , IL-6 and TNF- α with LPS in mRNA expressions (A, B and C, respectively). With IL-4 co-treatment, mRNA expression of IL-1 β was suppressed (A), while IL-6 and TNF- α expressed no significant differences compare to LPS only treated groups (B and C, respectively). PSLs and 1 % RGD-PSLs suppressed the expressions of LPS-induced IL-1 β and IL-6 (A and B, respectively), and 3 % and 5 % RGD-PSLs groups most suppressed expressions of IL-1 β , IL-6 and TNF- α of mRNA. After 12 h of liposome only treatment, mRNA expression of arg-1, FIZZ1 and YM-1, have significantly increased in IL-4 treated groups compare to other experimental groups (E, F and G, respectively). Also among the experimental groups 3 % RGD-PSLs have significantly increased the mRNA expression of the cytokines.

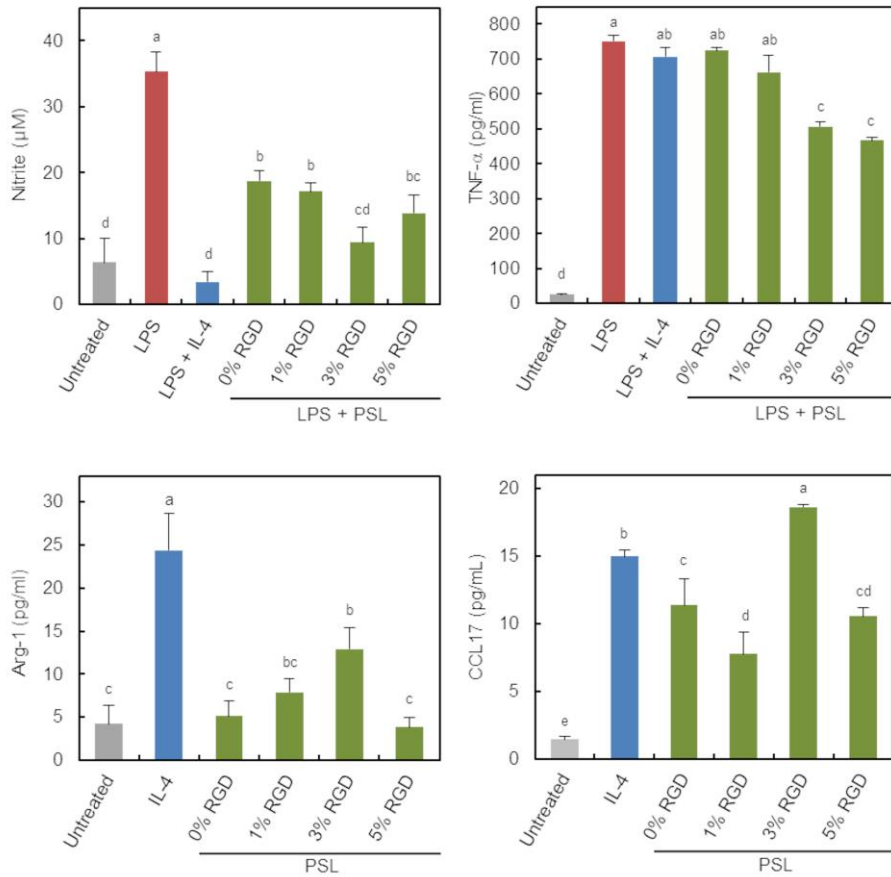


Figure 5. BMDM treated with the liposomes in two different conditions; Liposome co-treatment with LPS for 12 h and liposome only for 12 h. The results showed increase in secretion of NO and TNF- α (A and B, respectively).

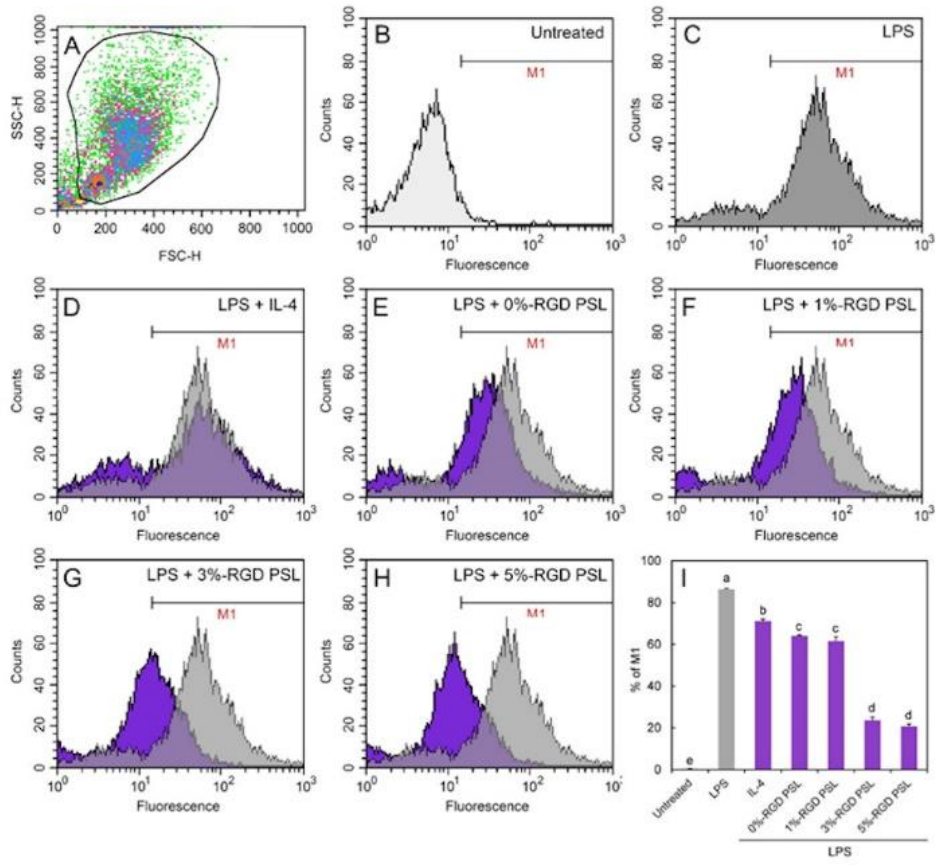
The nitric oxide secretion was suppressed with 3 % RGD-PSLs with no significant difference to the negative control group. For TNF- α ELISA, 3 % and 5 % RGD-PSLs showed effective in suppression of the cytokine secretion.

3.1.2 Flow Cytometry and Immunofluorescence

To evaluate the polarization state of BMDM, the cells were stained with CD68, CD86 and CD206. As shown in figure 6, BMDM were

successfully polarized to M1 macrophages with LPS treatment (86.29 ± 0.50) (Fig. 6. C). However, in 3 % and 5 % RGD-PSLs groups LPS-induced M1 macrophage polarizations were significantly suppressed (22.04 ± 1.45 % and 20.77 ± 1.07 %, respectively) (Fig. 6. G and H, respectively), while 0% and 1% RGD-PSLs showing similar polarization level (71.17 ± 0.94 % and 64.04 ± 0.38 %, respectively) to LPS + IL-4 co-treated group (Fig. 6. E and F, respectively). The immunofluorescence images also confirmed the results from flow cytometry analysis. The fluorescence of CD 86 (red) were suppressed with 0 %, 1 %, 3 % and 5 % RGD-PSLs (Fig. 6. J).

The flow cytometry and immunofluorescence results RGD-PSLs only treated BMDM were analyzed with CD 206. The results confirmed M2 polarization of BMDM with 3 % RGD-PSLs (48.10 ± 0.93 %) (Fig. 7. F). 3 % RGD-PSLs showed higher level of M2 macrophage polarization than IL-4 treated group (35.64 ± 3.30 %) and among the other experimental groups (Fig. 7. H). The immunofluorescence images also confirmed the results from flow cytometry analysis. The fluorescence of CD 206 (red) were enhanced in 3 % RGD-PSLs compare to other experimental groups (Fig. 7. I).



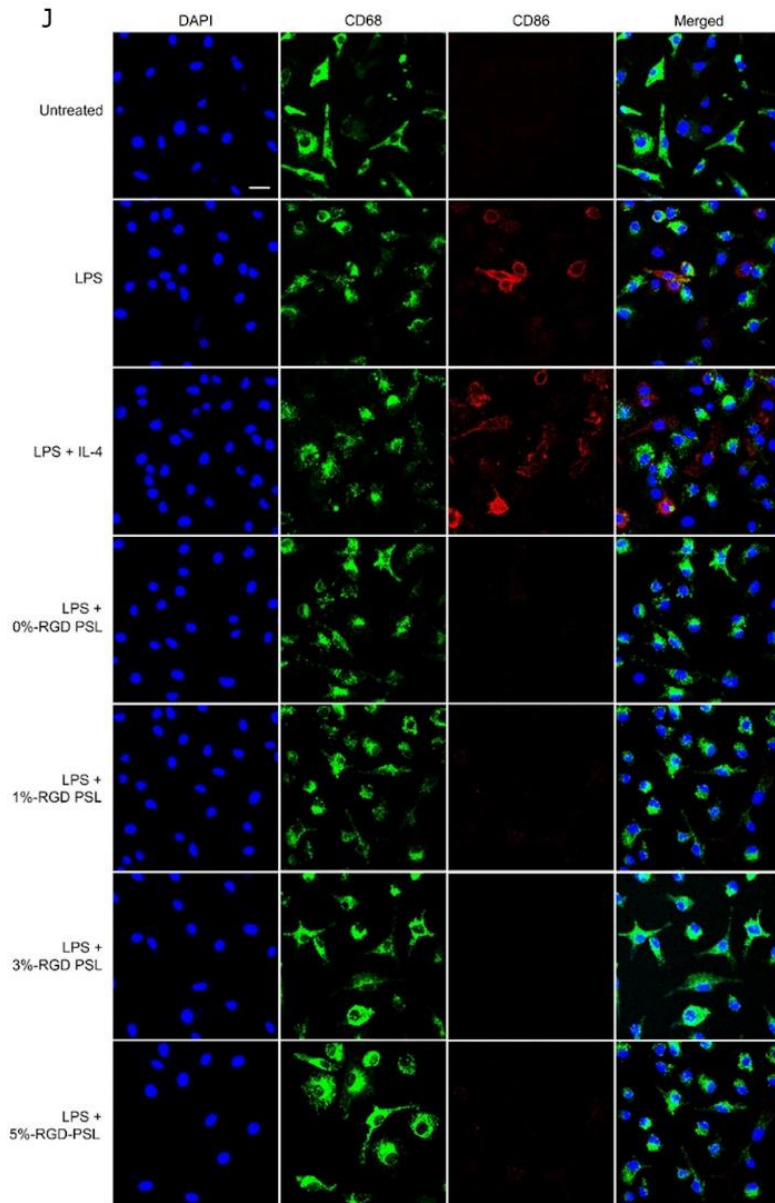
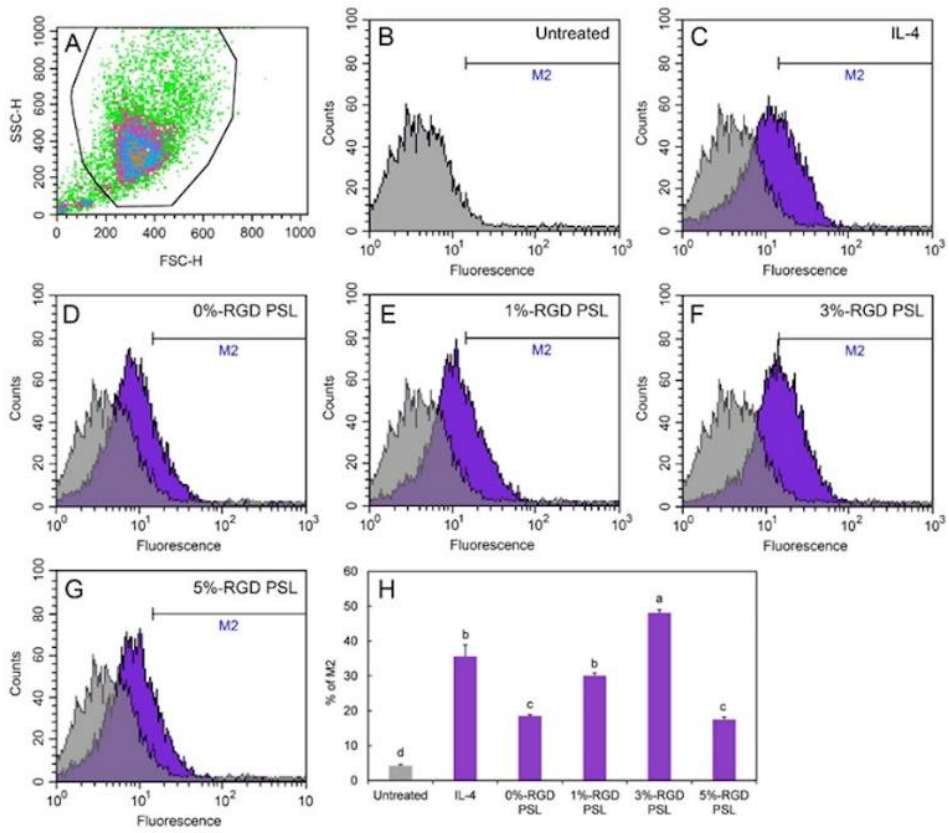


Figure 6. Flow cytometry analysis of LPS-induced BMDM treated with RGD-PSLs (A, B, C, D, E, F, G, H and I). BMDM were successfully polarized to M1 macrophages with LPS treatment (C). 3 % and 5 % RGD-PSLs significantly suppressed LPS-induced M1 macrophages (G and H, respectively). 0 % and 1 % RGD-PSLs showed similar level of M1 macrophage polarization (E and F, respectively) to LPS + IL-4 co-treated group (D). The immunofluorescence images of LPS- induced BMDM treated with RGD-PSLs show suppressed CD86 fluorescence (red) in 0 %, 1 %, 3 % and 5 % RGD-PSLs groups (J).



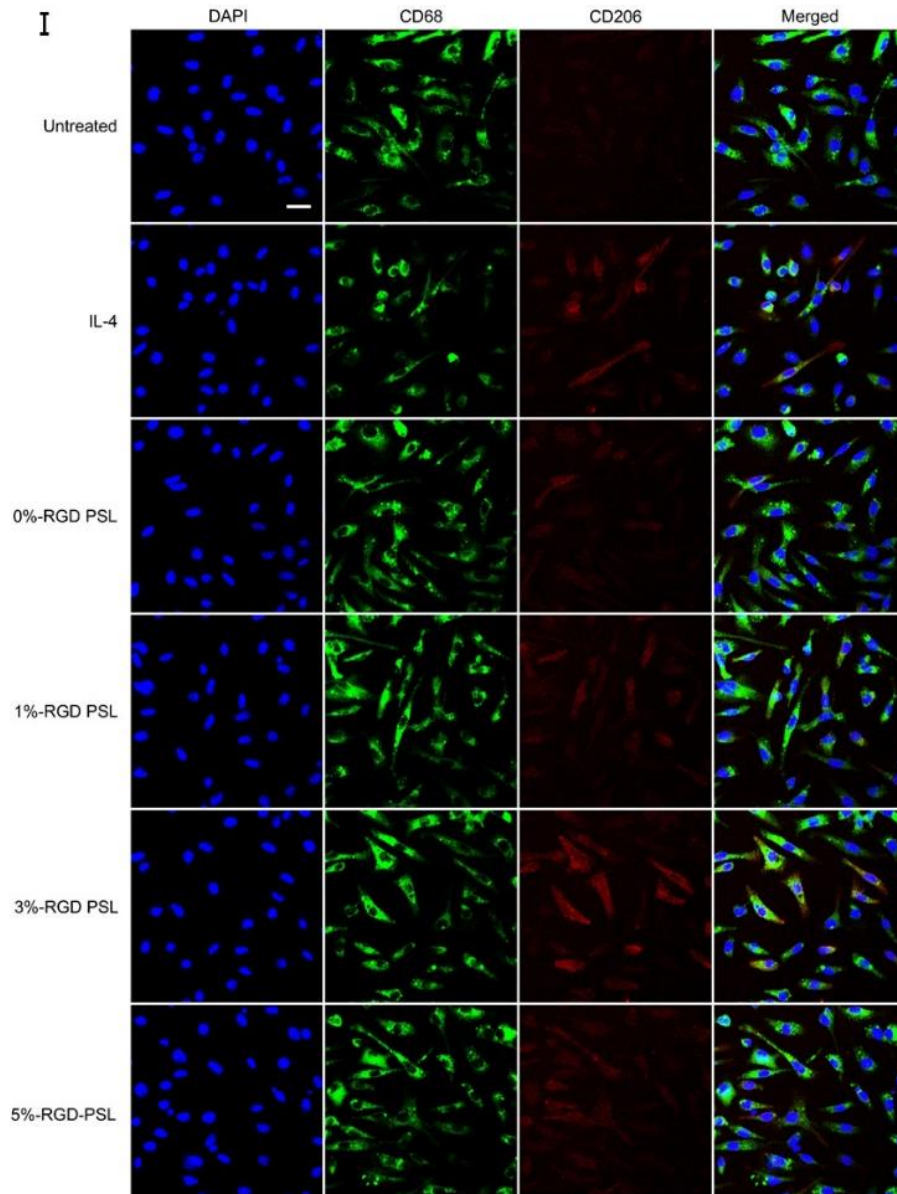


Figure 7.

Flow cytometry analysis of BMDM treated with RGD-PSLs (A, B, C, D, E, F, G and H). 3 % RGD-PSLs significantly enhanced M2 polarization of BMDM (F). The enhancement was higher than IL-4 treated group (H). The immunofluorescence images of BMDM treated with RGD-PSLs also show enhancement of CD 206 (red) fluorescence in 3 % RGD-PSLs group compare to other experimental groups (I).

3.1.3 Liposome Uptake by BMDM

As the RGD-motif play a key role in binding the PS of apoptotic cells and the integrin of macrophages induce phagocytosis, we hypothesized that by surface-grafting PSLs with RGD will enhance the liposome uptake by BMDM. To address this hypothesis, BMDM were incubated with TRITC-DHPE-labeled RGD-PSLs for 3 h. As shown in figure 8, 3% RGD-PSLs showed highest level of liposome uptake ($42.68 \pm 2.88\%$) and 0% and 1% RGD-PSLs showed lowest ($6.14 \pm 1.60\%$ and $8.20 \pm 1.22\%$, respectively) (Fig. 8. B).

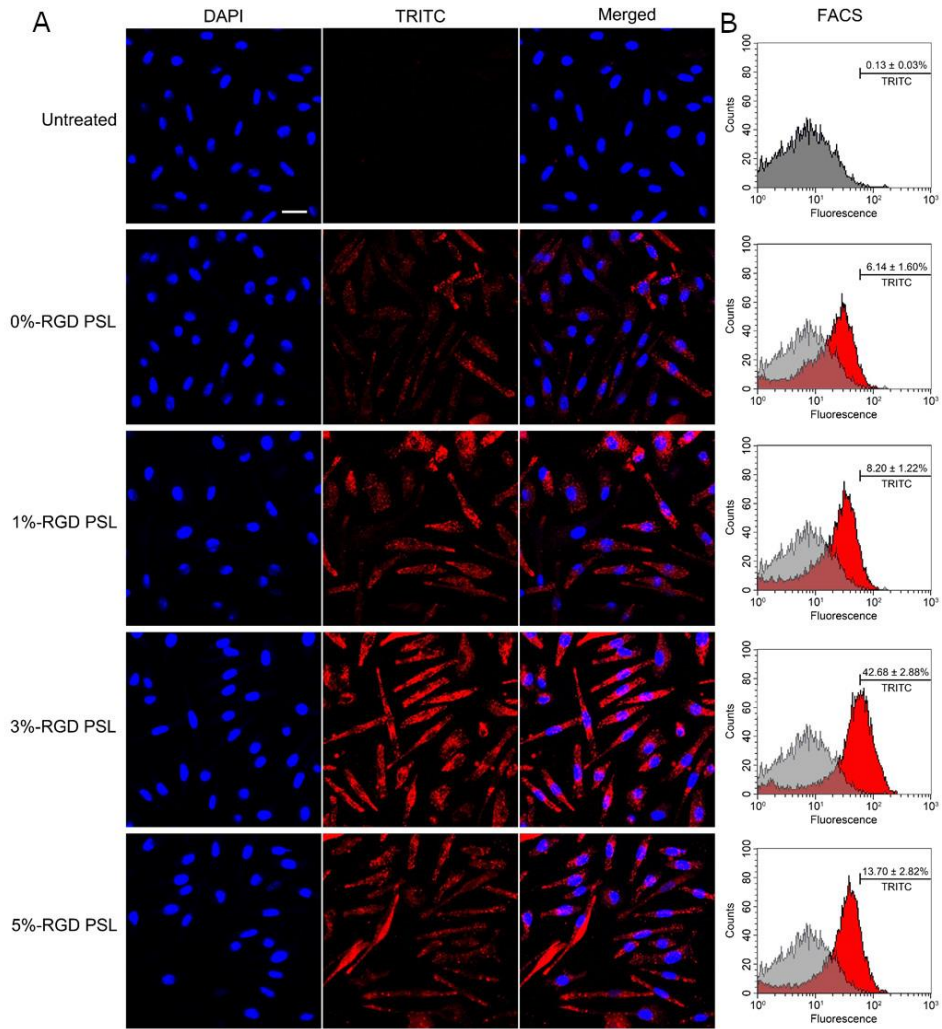


Figure 8. Macrophage uptake of RGD-PSLs labeled with TRITC-DHPE. 3 % RGD-PSLs show highest level of liposome uptake ($42.68 \pm 2.88\%$) and 0 % and 1 % RGD-PSLs showed lowest ($6.14 \pm 1.60\%$ and $8.20 \pm 1.22\%$, respectively) (B).

3.1.4 Tissue Ingrowth and Fibrous Encapsulation

To observe the effect of RGD-PSLs on wound healing and tissue regeneration, liposome entrapped alginate-gelatin matrix-embedded PVA were subcutaneously implanted in rats. After one and four weeks PVA and surrounding tissues were harvested and sectioned for Masson's trichrome staining. After one week, most of the alginate

and gelatin matrix have been degraded, and some pieces of debris were seen within the PVA. Therefore, it is certain that the liposomes had been observed to the surrounding tissues. Using a software (ImageJ, National Institute of Health, USA), total areas of each PVA were measured and the area of tissue ingrowth were measured for percentage of tissue ingrowth calculation (Fig. 9. A). The average tissue ingrowth in 3 % RGD-PSL showed highest percentage tissue ingrowth ($46.47 \pm 14.41 \%$), while 0 % RGD-PSL group ($15.24 \pm 7.67 \%$) was not significantly different to the control and carrageenan groups ($17.65 \pm 7.26 \%$ and $20.55 \pm 7.19 \%$, respectively) (Fig. 9. B). The effect of RGD-PSLs on fibrous encapsulations were analyzed after four weeks (Fig. 10). The thickness of fibrous capsule in carrageenan group showed thickest ($152.43 \pm 18.67 \mu\text{m}$), while control, PSLs and 3 % RGD-PSLs showed thinner fibrous capsule ($75.58 \pm 30.67 \mu\text{m}$, $78.53 \pm 21.76 \mu\text{m}$ and $71.06 \pm 27.06 \mu\text{m}$, respectively) with no significant differences within the groups (Fig. 10. B).

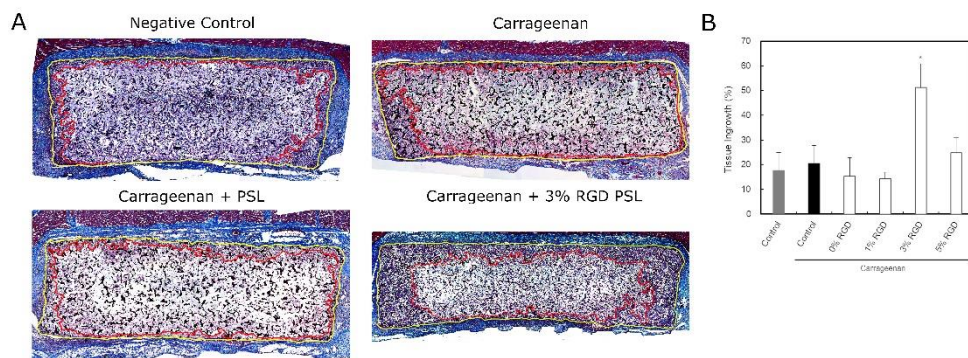


Figure 9. Tissue sections of PVA after one week of subcutaneous implantation. The surrounding tissues were stained with Masson's trichrome. The average tissue ingrowth in 3 % RGD-PSL showed highest percentage tissue ingrowth ($46.47 \pm 14.41 \%$), while 0% RGD-PSL group ($15.24 \pm 7.67 \%$) was not significantly different

to the control and carrageenan groups ($17.65 \pm 7.26 \%$ and $20.55 \pm 7.19 \%$, respectively)

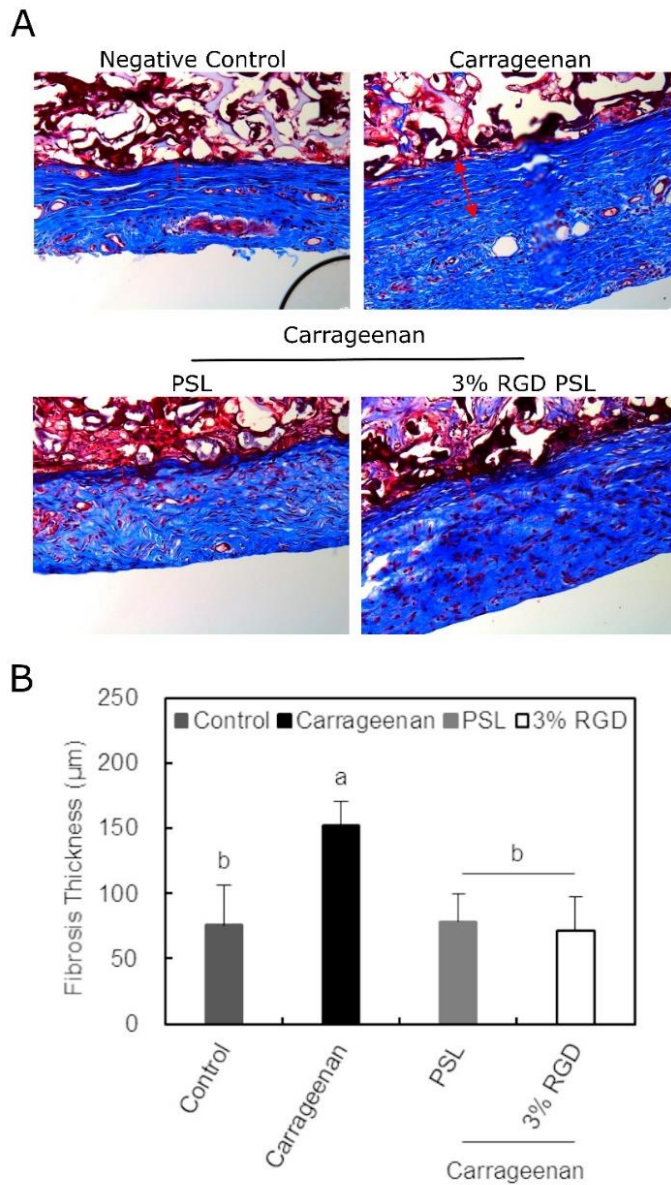


Figure 10. Fibrous encapsulation analysis after four week of implantation (A). The thickness of fibrous capsule in carrageenan group showed thickest ($152.43 \pm 18.67 \mu\text{m}$), while control, PSLs and 3 % RGD-PSLs showed thinner fibrous capsule ($75.58 \pm 30.67 \mu\text{m}$, $78.53 \pm 21.76 \mu\text{m}$ and $71.06 \pm 27.06 \mu\text{m}$, respectively) with no significant differences within the groups (B).

3.1.5 Polarization of Macrophages Recruited to Surrounding Tissues

To confirm the polarization of macrophages recruited to PVA, tissue sections of one week were stained with M1 and M2 markers (iNOS and arg-1, respectively) (Fig. 11. A and C, respectively). As shown in figure 11 B and D, average number of cells from each groups were quantified. The results from iNOS showed highest number of cells in carrageenan group (225.88 ± 41.38), while 3 % RGD-PSLs showed lowest number of cells (2.76 ± 185) which had no significantly difference with control group (0.88 ± 0.99). However, there were no significantly differences within the other experimental groups in arg-1 expression (Fig. 11. D).

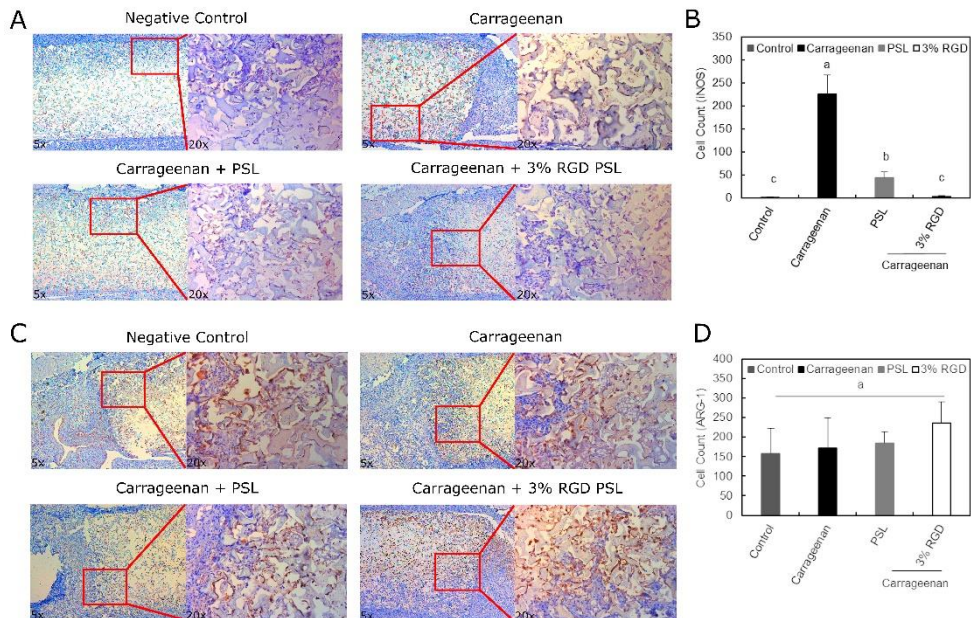


Figure 11. Tissue sections immunohistochemically stained with M1 and M2 markers (iNOS and arg-1, respectively) (A and C, respectively). Carrageenan group showed highest number of M1 macrophages (225.88 ± 41.38), while 3 % RGD-PSLs showed lowest number of the cells (2.76 ± 185). However, there were no significantly differences within the experimental groups in arg-1 expression.

3.2 Effect of PEG-PSLs Fibrous Capsule

3.2.2 The Size of Liposomes and the Spatial Disposition of PSLs in Alginate-Gelatin Mixture

The size of PSLs and PEG-PSLs ranged between 100 and 400nm (Fig. 12. A and B, respectively). Although the liposomes were sized with 400nm membrane filter, some particles were bigger than 400 nm. This is most likely due to the liposome aggregation or fusion after filtration. The mean and mode of PSL particle size were 230 ± 91.6 (SD) and 196.7 nm, respectively. Similarly, PEG-PSLs particles appeared to have a mean size of 224.4 ± 86.6 (SD), with a mode of 190.9 nm. The liposomes were used for the preparation of the liposome-alginate-gelatin mixture and covered MCE membranes. To confirm the homogeneously mixed liposomes in alginate-gelatin matrix, TRITC-labeled fluorescent PSLs in the alginate-gelatin layer were observed under a confocal microscope. As shown in figure 12 C, fluorescent dots were evenly distributed within the alginate-gelatin matrix. Therefore, it likely that PSLs were not significantly aggregated during the mixing process with matrices.

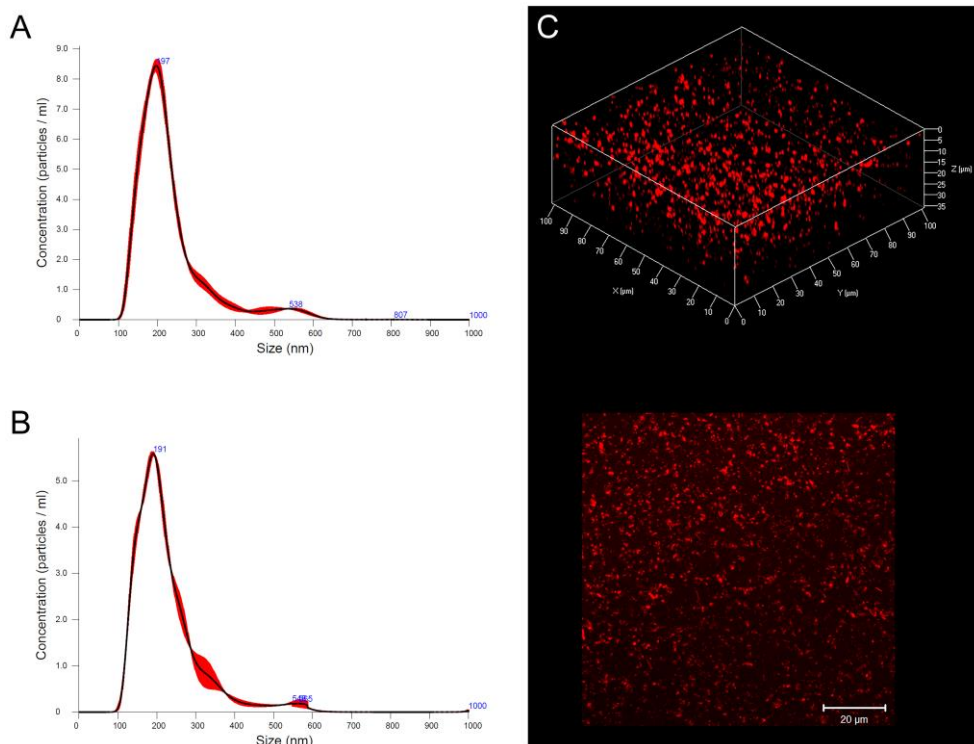


Figure 12. The size of PSLs and PEG-PSLs (A and B, respectively). The sizes of the liposomes ranged between 100 and 400 nm. Although the liposomes were sized with 400nm membrane filter, some particles were bigger than 400 nm. The mean and mode of PSL particle size were 230 ± 91.6 (SD) and 196.7 nm, respectively. Similarly, PEG-PSLs particles appeared to have a mean size of 224.4 ± 86.6 (SD), with a mode of 190.9 nm. The TRITC-labeled fluorescent PSLs show homogeneously mixed liposomes in alginate-gelatin matrix (C).

3.2.3 Effect of PEG-PSLs on TGF- β expression

To evaluate the effect of PEG-PSLs on TGF- β expression in macrophages, RAW 264.7 cells were co-treated with the liposomes and IL-4, and M2-inducing cytokines. As shown in figure 13, IL-4 increased TGF- β mRNA expression and protein secretion. After 12 h, PSLs inhibited IL-4-induced TGF- β mRNA expression (Fig. 13 A). However, the secretion of TGF- β protein was not affected by PSLs after 24 h of treatment (figure not include), suggesting the mRNA expression could have been temporarily inhibited. In contrast to PSLs,

PEG-PSLs inhibited both TGF- β mRNA expression and TGF- β protein secretion, completely preventing IL-4-induced expression of TGF- β .

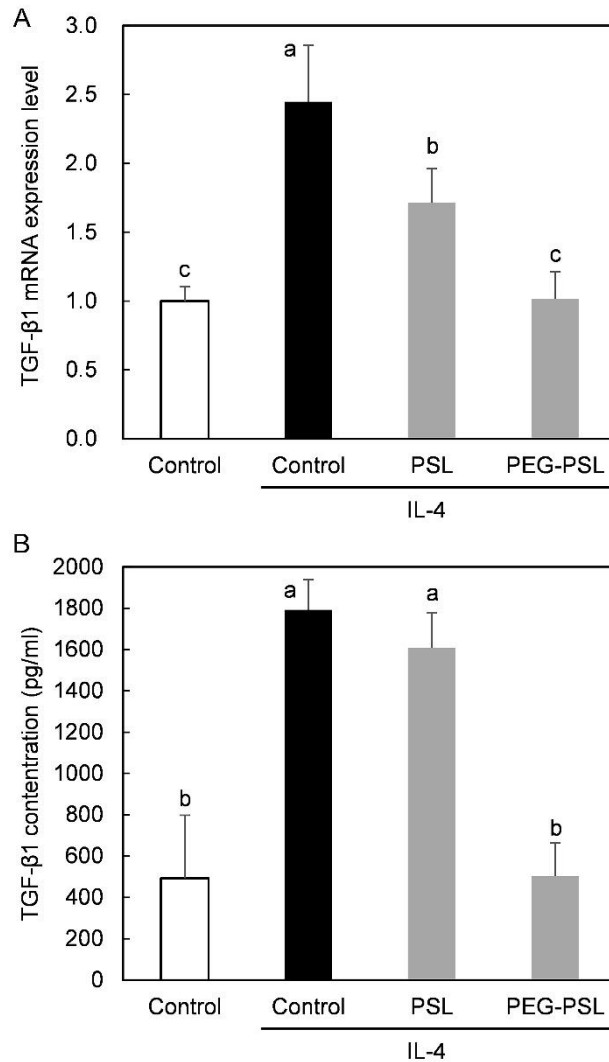


Figure 13. Effect of PEG-PSLs on TGF- β expression in macrophages. RAW 264.7 cells were co-treated with the liposomes and IL-4, and M2-inducing cytokines. IL-4 increased TGF- β mRNA expression and protein secretion. After 12 h, PSLs inhibited IL-4-induced TGF- β mRNA expression (A). In contrast to PSLs, PEG-PSLs inhibited both TGF- β mRNA expression and TGF- β protein secretion, completely preventing IL-4-induced expression of TGF- β (A and B, respectively).

3.2.4. Effect of PEG-PSLs on MGC formation

To investigate the involvement of the PEG-PSLs in FBGC formation, the inhibitory effect of PSLs and PEG-PSLs on IL-4-induced MGC formation was assessed. RAW 264.7 cells formed MGC in the presence of IL-4 for 48 h (Fig. 14. A). When the cells were co-treated with PSLs or PEG-PSLs and IL-4, the MGC formation was inhibited, and PEG-PSLs also interfered with IL-4-induced MGC formation (Fig. 14. B). In the co-treatment assay, the liposomes could not completely suppress the occurrence of MGC, and the degree of inhibition by PEG-PSLs was similar to the PSL-treated group. Pre-treatment with liposomes also inhibited IL-4-induced MGC formation (Fig. 14. C). There was no significant difference in the number of MGC between the PSLs and PEG-PSLs groups. We also performed pre-treatment and co-treatment together (pre/co-treatment). As shown in figure 14 D, the pre/co-treatment lead to the complete suppression of MGC formation in both PSLs and PEG-PSLs groups. However, no remarkable difference in the inhibitory effect was observed.

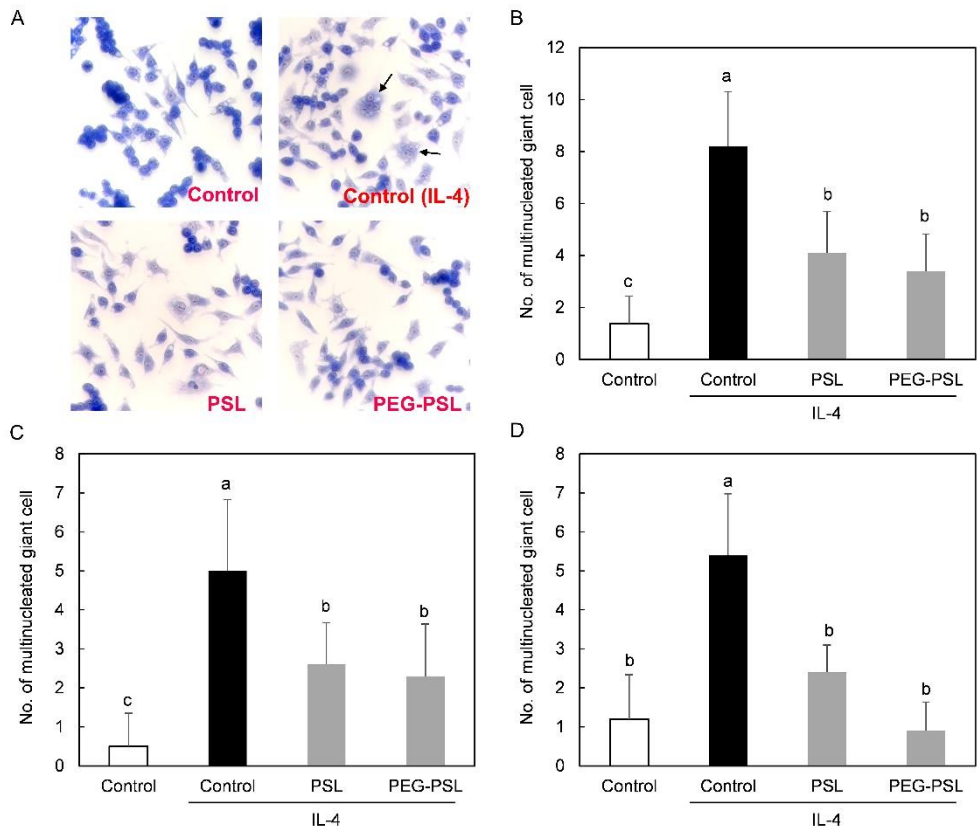


Figure 14. Effect of PEG-PSLs on MGC formation. RAW 264.7 cells formed MGC in the presence of IL-4 for 48 h (A). When the cells were co-treated with PSLs or PEG-PSLs and IL-4, the MGC formation was inhibited (B). However, the liposomes could not completely suppress the occurrence of MGC, and the degree of inhibition by PEG-PSLs was similar to the PSL-treated group. Pre-treatment with liposomes also inhibited IL-4-induced MGC formation (C). There was no significant difference in the number of MGC between the PSLs and PEG-PSLs groups. In pre/co-treatment of IL-4 and the liposomes, formation of MGC were completely suppressed in both PSLs and PEG-PSLs groups. However, no remarkable difference in the inhibitory effect was observed.

3.2.5. Macrophage attachment to alginate-gelatin matrix

Attachment of macrophages to alginate-gelatin matrices were analyzed with live/dead cell viability assay in vitro. The fluorescence

images show that the live cells are evenly spread and attached to the surface of the matrices (Fig. 15. A). Moreover, there were no significant differences in the average number of cell attachment among the experimental groups; control group: 181.33 ± 15.18 , PSL group: 203.33 ± 15.31 and PEG-PS group: 205.00 ± 15.10 (Fig. 15. B).

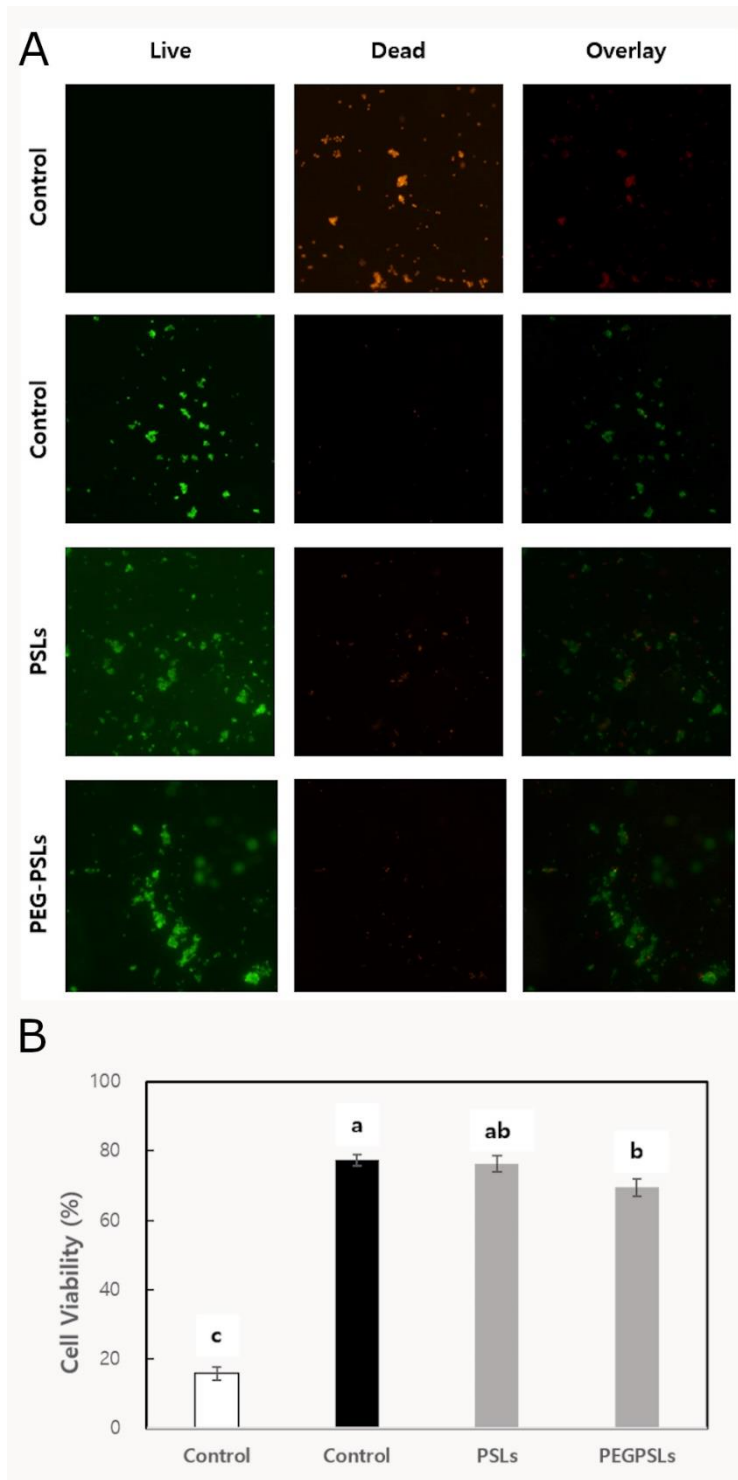


Figure 15. Macrophage attachment to alginate-gelatin matrix analysis with live/dead cell viability assay. The fluorescence images show that the live cells are evenly spread and attached to the surface of the matrices (A). there were no

significant differences in the average number of cell attachment among the experimental groups; control group: 181.33 ± 15.18 , PSL group: 203.33 ± 15.31 and PEG-PS group: 205.00 ± 15.10 (B).

3.2.6. Histological observation and fibrous encapsulation analysis

To observe the effect of PEG-PSLs on fibrous encapsulation, MCE membranes coated with the liposome-alginate-gelatin matrix were subcutaneously implanted in rats. After four weeks, the membranes and the surrounding tissues were harvested and examined for histological analysis. Histological observations showed that the MCE membranes were surrounded by fibrous capsules and subcutaneous tissues after four weeks (Fig. 16 and 17 A). Most of the alginate-gelatin matrix have been degraded, and some pieces of debris, presumably biodegraded residues of the matrix, were shown around the MCE membranes. Therefore, the majority of the liposomes had certainly been released from the alginate-gelatin matrix into surroundings. H&E staining showed that the tissues adjacent to the implanted membranes had been mostly remodeled, with fibroblasts and collagen fibers dominating the remodeled tissue area (Fig. 16). Blood vessels were also frequently observed, indicating the occurrence of tissue repair most likely due to the tissue damage from the implantation and foreign body reaction. Macrophages were observed mostly on the surface of the membranes and randomly on small pieces of debris.

Fibrous encapsulation was analyzed in tissue section stained with Masson's trichrome stain, in which collagenous fibrous capsule was easily discernable (Fig. 17. A). Figure 17 B shows the average width

of the fibrous capsules formed on the same side as the alginate-gelatin matrices. The thickness of fibrous capsules in the PSL group (159 ± 39.4 nm) was not significantly different to the control group (130.8 ± 28.8 nm), while the PEG-PSL group (66.9 ± 27.6) showed thinner fibrous capsules than the control and PS groups. We also took PEG-PC into consideration to examine whether PEG without PS would have effect on the fibrous capsule formation. In contrast to PEG-PS, the PEG-PC group showed capsule thickness (119.2 ± 46.0) similar to the control group. Hence, both PEG and PS were needed to reduce fibrous encapsulation of the MCE membranes.

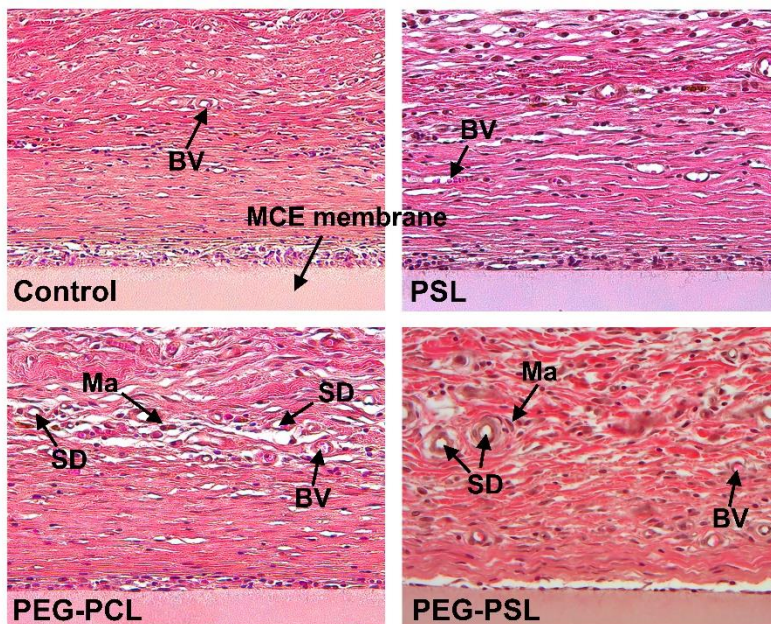


Figure 16. H&E staining of tissue sections around MCE membrane. Most of the alginate-gelatin matrix have been degraded, and some pieces of debris, presumably biodegraded residues of the matrix, were shown around the MCE membranes. the tissues adjacent to the implanted membranes had been mostly remodeled, with fibroblasts and collagen fibers dominating the remodeled tissue area. Blood vessels were also frequently observed, indicating the occurrence of tissue repair most likely due to the tissue damage from the implantation and foreign

body reaction. Macrophages were observed mostly on the surface of the membranes and randomly on small pieces of debris.

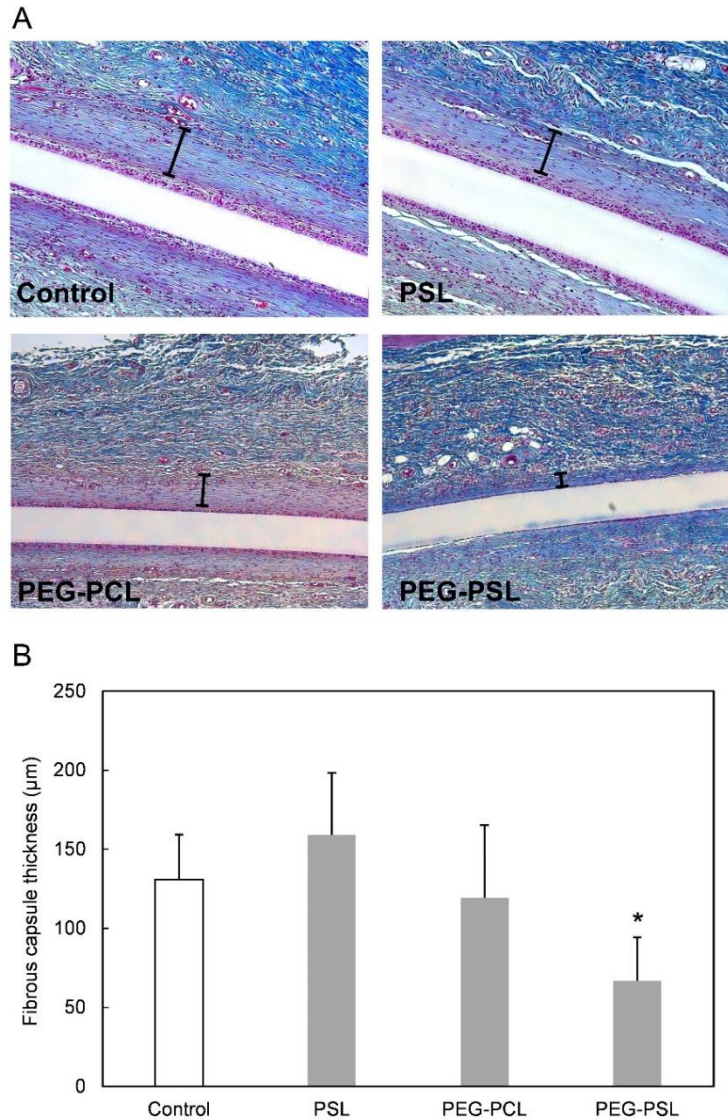


Figure 17. Tissue sections stained with Masson's trichrome staining for fibrous encapsulation analysis. The thickness of fibrous capsules in the PSL group (159 ± 39.4 nm) was not significantly different to the control group (130.8 ± 28.8 nm), while the PEG-PSL group (66.9 ± 27.6) showed thinner fibrous capsules than the control and PS groups (B). In contrast to PEG-PS, the PEG-PC group showed capsule thickness (119.2 ± 46.0) similar to the control group.

Chapter 4. Discussion

The cytokines secreted from anti-inflammatory M2 macrophages are known to promote wound healing and participate in bone formations (Gu et al., 2017; Kim et al., 2016; Munoz et al., 2020). Study by Wang et al. 2017A have reported that macrophages cultured on anodic oxidized nanotubular titanium discs at 20V induced polarization to M2 phenotypes which enhanced osteogenesis of osteoblastic cells (Wang et al., 2017A). For this reason, various attempts have been done to modulate inflammatory response of the macrophages by increasing the anti-inflammatory activities of the macrophages. In study by Ji et al. (2019), anemarrhena asphodeloides extract was introduced to express anti-inflammatory effect by inhibiting the expression of pro-inflammatory cytokines such as IL-1beta, IL-6, TNF-alpha and COX-2 on RAW 264.7 cells (Ji et al., 2019). In another study, celecoxib, commonly used COX-2 inhibitor for anti-inflammatory therapy, was synthesized with folate and BOC-glycine to construct folate-glycine-celecoxib. The folate on the folate-glycine-celecoxib directly targeted folate receptor on macrophages to enhance the anti-inflammatory effect and reduce adverse effect of the conventional celecoxib. The results showed that folate-glycine-celecoxib expressed increase in suppression effect on LPS-induced nitric oxide (NO) compared to the conventional celecoxib in RAW 264.7 cells (Li et al., 2017). However, these strategies only showed suppressive effect on LPS-induced pro-inflammation and did not show any effect on increase in anti-inflammatory effect. Also the celecoxib used in the study by Li et al., (2016), is non-steroidal anti-inflammatory drugs, which can increase cardiovascular risks and is not macrophage-specific. For this reason PSLs makes most relevant

strategy for enhancing M2 polarization of macrophages.

PS of apoptotic cells express “eat-me” signals promoting engulfment of the apoptotic cell by phagocytosis (Fadok et al., 2000; Kourtzelis et al., 2020) and increase secretion of anti-inflammatory cytokines (Borisenko et al., 2003). For this reason, PSLs are an appropriate approach to target macrophages and induce anti-inflammatory macrophages. However, to enhance the polarization of macrophages to M2 by PSLs, we surface-grafted the PSLs with RGD. RGD on RGD-PSLs were to mimic the RGD-motif of MFG-E8 and enhance M2 polarization of macrophages by the liposomes directly binding to $\alpha v\beta 3/\alpha v\beta 5$ -integrins of macrophages. RGD on RGD-PSLs binding to the $\alpha v\beta 3/\alpha v\beta 5$ -integrins results activation Rac1 inducing cytoskeletal remodeling in macrophage promote phagocytosis of the liposomes.

In this study, we have used three different mole percentages of RGDs grafted on PSLs. The results showed that 3 % RGD-PSLs suppressed LPS-induced M1 macrophage polarization and enhanced polarization to M2 macrophages in both mRNA and protein levels (Fig. 4 and 5). The M2 polarization effect of 3 % RGD-PSLs was confirmed with flow cytometry and immunofluorescence (Fig. 7). These results partially correlate with the results from the animal experiment. The histological analysis of animal experiment showed that after one week of subcutaneous implant, 3 % RGD-PSLs resulted highest percentage of tissue ingrowth (Fig. 9). Also the immunohistochemical analysis showed, 3 % RGD-PSLs suppressed number of M1 macrophages significantly different to other groups (Fig. 11. B). These results show that only certain mole percentages of RGD-PSLs are effective in M2 polarization of macrophages. The exact biological mechanism needs to be further investigated but it can be speculated that certain degree of bindings between the integrins/receptors on

macrophages and RGD/PS on liposomes are required for enhancing phagocytosis effectively. However, the results also imply that suppression of pro-inflammatory cytokines is also important for tissue regeneration. As shown in the figure 11 D, immunohistochemical analysis of M2 macrophages showed no significant differences between the experimental groups after one week, while significantly reducing the thickness of carrageenan-induced fibrous capsule in PSLs and 3 % RGD-PSLs groups after four weeks (Fig. 10. D). From these results it can be perceived the importance of attenuating the M1 macrophage polarization for inhibiting fibrous capsule (Wynn & Vannella, 2016).

In our previous study, we have reported that PSLs induced TGF- β production in macrophages and the PS activity was inhibited by grafting liposomes with PEG (Quan et al., 2017). To reduce the dysfunction of implanted medical devices, minimizing fibrous capsule around the devices is important. For this reason, there have been number of studies done to reduce fibrous capsule by using TGF- β inhibitors (Park et al., 2015; Sevilla et al., 2018; Wang et al., 2017B). These studies indicate that the inhibition of TGF- β is an appropriate target for inhibiting fibrous capsule. Because M2 macrophages produce considerable amount of TGF- β , it is expected that targeting the suppression of TGF- β produced from macrophages can reduce fibrous capsule. The results from in vitro showed that PEG-PSLs inhibited TGF- β production in IL-4-induced M2 macrophages (Fig. 13). The results imply that the PEG-PSLs prevented activity of M2 macrophages or polarization of macrophages to M2 phenotype. However, it is clearly not understood how the PEG-PSLs inhibit M2 polarization of macrophages. It can be speculated that PEG-PSLs might interfere with binding between IL-4 and IL-4 receptor via a

masking effect, or the liposomes might act on the intracellular signal transduction leading to M2 polarization.

In this study, we also considered the possibility of the involvement of FBGCs in fibrous encapsulation. Previous studies have shown the expression of TGF- β from biomaterial-derived FBGCs (Hernandez-Pando et al., 2000; Higgins et al., 2009). FBGCs are formed by the fusion of macrophages and known to appear on the surface of implanted biomaterials. However, as shown in figure 14, both PSLs and PEG-PSLs prevented MGC formation, while only PEG-PLS showed effect of reducing fibrous capsule (Fig. 17). Because PSLs and PEG-PCLs did not attenuate fibrous capsule, it is certain that both PS and PEG are required to for PEG-PSLs to effectively reduce fibrous capsule formation. The results from this study demonstrate that PEG-PSLs suppressed the expression of TGF- β by inhibiting the M2 macrophage polarization. Because TGF- β recruit fibroblasts and differentiate them to myofibroblast, which produce collagen to form fibrosis, the inhibition of TGF- β production by PEG-PSLs is thought to reduce fibrous capsule in vivo.

In a study by Helming et al. (2009), they have explained the mechanism underlying the suppression of MGC formation by PSLs (Helming et al., 2009). MGC are formed by the fusion of macrophages, and the binding of PS with CD36 on the cell surface is known to be involved in cell fusion. The binding of endogenous PS with CD36 can be interfered by PSLs through competitive inhibition, which results in the failure of cell fusion. Our results suggest that PEG-PSLs also interfered with the binding between CD36 and endogenous PS. There was no significant difference between PSLs and PEG-PSLs in the degree of inhibition of MGC formation, regardless of treatment time (ie. pre-treatment and co-treatment). Therefore, it can be assumed

that the fibrous capsule inhibition by PEG-PSLs is not by the suppression of FBGC formation.

RGD-PSLs and PEG-PSLs were supposed to encounter macrophage to exhibit their effects in animal models. The liposomes should be timely released from the matrix as macrophages appear at certain period of time after implantation. For this reason, it can be speculated that the alginate-gelatin matrix was properly degraded after implantation in these studies. However, prolonged existence of liposomes and modulation of macrophage polarization can raise safety concerns. In study by Shull et al. (1992), they have reported that homogeneous deletion of TGF- β resulted in multi-organ inflammation and death of mice (Shull et al., 1992). Therefore, a timely and proper level of macrophage polarization is needed for optimizing the effect of liposomes and further study is needed to establish valid conditions for matrices to entrap and release the liposomes properly.

Chapter 5. Conclusion

Macrophage polarization possesses a key role in inflammatory response. In this study we have demonstrated modulation of macrophage polarization by surface-grafting of PSLs with RGD and PEG. 3 % RGD-PSLs showed increase in anti-inflammatory activities of macrophages by promoting engulfment of the liposomes through RGD and integrin binding. This has led to increase in tissue regeneration in in vivo experiment. Also PEG-PSLs showed inhibitory effect in TGF- β secretion and FBGC formation in in vitro and suppressed foreign body induced fibrous capsule in in vivo. Because anti-inflammatory M2 macrophages participated in activation of MSC to osteoblastic cells, 3 % RGD-PSLs show potential in clinical use for osteogenesis and PEG-PSLs possibility for use in implanted medical devices to reduce fibrous capsule.

References

- Anderson, J. M., Rodriguez, A., & Chang, D. T. (2008, Apr). Foreign body reaction to biomaterials. *Semin Immunol*, *20*(2), 86–100.
- Aramaki, Y., Nitta, F., Matsuno, R., Morimura, Y., & Tsuchiya, S. (1996, Mar 7). Inhibitory effects of negatively charged liposomes on nitric oxide production from macrophages stimulated by LPS. *Biochemical and Biophysical Research Communications*, *220*(1), 1–6.
- Borisenko, G. G., Matura, T., Liu, S. X., Tyurin, V. A., Jianfei, J., Serinkan, F. B., & Kagan, V. E. (2003, May 1). Macrophage recognition of externalized phosphatidylserine and phagocytosis of apoptotic Jurkat cells--existence of a threshold. *Arch Biochem Biophys*, *413*(1), 41–52.
- Brisette, M. J., Lepage, S., Lamonde, A. S., Sirois, I., Groleau, J., Laurin, L. P., & Cailhier, J. F. (2012). MFG-E8 released by apoptotic endothelial cells triggers anti-inflammatory macrophage reprogramming. *PLoS One*, *7*(4), e36368.
- Brodbeck, W. G., & Anderson, J. M. (2009, Jan). Giant cell formation and function. *Current Opinion in Hematology*, *16*(1), 53–57.
- Callahan, M. K., Halleck, M. S., Krahling, S., Henderson, A. J., Williamson, P., & Schlegel, R. A. (2003, Nov). Phosphatidylserine expression and phagocytosis of apoptotic thymocytes during differentiation of monocytic cells. *J Leukoc Biol*, *74*(5), 846–856.
- Cho, D. I., Kim, M. R., Jeong, H. Y., Jeong, H. C., Jeong, M. H., Yoon, S. H., Kim, Y. S., & Ahn, Y. (2014, Jan 10). Mesenchymal stem cells reciprocally regulate the M1/M2 balance in mouse bone marrow-derived macrophages. *Exp Mol Med*, *46*, e70.
- Das, A., Ghatak, S., Sinha, M., Chaffee, S., Ahmed, N. S., Parinandi, N. L., Wohleb, E. S., Sheridan, J. F., Sen, C. K., & Roy, S. (2016, Jun 15). Correction of MFG-E8 Resolves Inflammation and Promotes Cutaneous Wound Healing in Diabetes. *J Immunol*, *196*(12), 5089–5100.
- Fadok, V. A., Bratton, D. L., Rose, D. M., Pearson, A., Ezekewitz, R. A., & Henson, P. M. (2000, May 4). A receptor for phosphatidylserine-

specific clearance of apoptotic cells. *Nature*, 405(6782), 85-90.

Fuller, A. D., & Van Eldik, L. J. (2008, Dec). MFG-E8 regulates microglial phagocytosis of apoptotic neurons. *J Neuroimmune Pharmacol*, 3(4), 246-256.

Gong, L., Zhao, Y., Zhang, Y., & Ruan, Z. (2016, Winter). The Macrophage Polarization Regulates MSC Osteoblast Differentiation in vitro. *Ann Clin Lab Sci*, 46(1), 65-71.

Gu, Q., Yang, H., & Shi, Q. (2017, Jul). Macrophages and bone inflammation. *J Orthop Translat*, 10, 86-93.

Harel-Adar, T., Ben Mordechai, T., Amsalem, Y., Feinberg, M. S., Leor, J., & Cohen, S. (2011, Feb 1). Modulation of cardiac macrophages by phosphatidylserine-presenting liposomes improves infarct repair. *Proc Natl Acad Sci U S A*, 108(5), 1827-1832.

Helming, L., Winter, J., & Gordon, S. (2009, Feb 15). The scavenger receptor CD36 plays a role in cytokine-induced macrophage fusion. *J Cell Sci*, 122(Pt 4), 453-459.

Hernandez-Pando, R., Bornstein, Q. L., Aguilar Leon, D., Orozco, E. H., Madrigal, V. K., & Martinez Cordero, E. (2000, Jul). Inflammatory cytokine production by immunological and foreign body multinucleated giant cells. *Immunology*, 100(3), 352-358.

Higgins, D. M., Basaraba, R. J., Hohnbaum, A. C., Lee, E. J., Grainger, D. W., & Gonzalez-Juarrero, M. (2009, Jul). Localized immunosuppressive environment in the foreign body response to implanted biomaterials. *Am J Pathol*, 175(1), 161-170.

Hinz, B. (2007, Mar). Formation and function of the myofibroblast during tissue repair. *J Invest Dermatol*, 127(3), 526-537.

Ji, K. Y., Kim, K. M., Kim, Y. H., Im, A. R., Lee, J. Y., Park, B., Na, M., & Chae, S. (2019, Jun). The enhancing immune response and anti-inflammatory effects of *Anemarrhena asphodeloides* extract in RAW 264.7 cells. *Phytomedicine*, 59, 152789.

Kenneth Ward, W. (2008, Sep). A review of the foreign-body response to

subcutaneously-implanted devices: the role of macrophages and cytokines in biofouling and fibrosis. *J Diabetes Sci Technol*, 2(5), 768-777.

Kim, Y. K., Chen, E. Y., & Liu, W. F. (2016). Biomolecular strategies to modulate the macrophage response to implanted materials. *Journal of Materials Chemistry B*, 4(9), 1600-1609.

Klibanov, A. L., Maruyama, K., Torchilin, V. P., & Huang, L. (1990, Jul 30). Amphipathic polyethyleneglycols effectively prolong the circulation time of liposomes. *FEBS Lett*, 268(1), 235-237.

Kourtzelis, I., Hajishengallis, G., & Chavakis, T. (2020, Mar 31). Phagocytosis of Apoptotic Cells in Resolution of Inflammation. *Frontiers in Immunology*, 11.

Kusunoki, R., Ishihara, S., Aziz, M., Oka, A., Tada, Y., & Kinoshita, Y. (2012). Roles of milk fat globule-epidermal growth factor 8 in intestinal inflammation. *Digestion*, 85(2), 103-107.

Levchenko, T. S., Rammohan, R., Lukyanov, A. N., Whiteman, K. R., & Torchilin, V. P. (2002, Jun 20). Liposome clearance in mice: the effect of a separate and combined presence of surface charge and polymer coating. *Int J Pharm*, 240(1-2), 95-102.

Li, Y. Q., Xiao, Y., & Yin, Z. N. (2017, Apr). Enhanced Anti-Inflammatory Efficacy Through Targeting to Macrophages: Synthesis and In Vitro Evaluation of Folate-Glycine-Celecoxib. *Aaps Pharmscitech*, 18(3), 729-737.

Mosser, D. M., & Edwards, J. P. (2008, Dec). Exploring the full spectrum of macrophage activation. *Nat Rev Immunol*, 8(12), 958-969.

Munoz, J., Akhavan, N. S., Mullins, A. P., & Arjmandi, B. H. (2020, Sep 30). Macrophage Polarization and Osteoporosis: A Review. *Nutrients*, 12(10).

Myers, K. V., Amend, S. R., & Pienta, K. J. (2019, May 14). Targeting Tyro3, Axl and MerTK (TAM receptors): implications for macrophages in the tumor microenvironment. *Mol Cancer*, 18(1), 94.

- Naeini, M. B., Bianconi, V., Pirro, M., & Sahebkar, A. (2020). The role of phosphatidylserine recognition receptors in multiple biological functions. *Cell Mol Biol Lett*, *25*, 23.
- Otusuka, M., Goto, K., Tsuchiya, S., & Aramaki, Y. (2005). Phosphatidylserine-Specific Receptor Contributes to TGF- β Production in Macrophages through a MAP Kinase, ERK. *Biol. Pharm. Bull.*, *28*(9), 1107-1110.
- Park, S., Park, M., Kim, B. H., Lee, J. E., Park, H. J., Lee, S. H., Park, C. G., Kim, M. H., Kim, R., Kim, E. H., Heo, C. Y., & Choy, Y. B. (2015, Feb 28). Acute suppression of TGF- β with local, sustained release of tranilast against the formation of fibrous capsules around silicone implants. *J Control Release*, *200*, 125-137.
- Quan, H., Park, H. C., Kim, Y., & Yang, H. C. (2017, May). Modulation of the anti-inflammatory effects of phosphatidylserine-containing liposomes by PEGylation. *J Biomed Mater Res A*, *105*(5), 1479-1486.
- Ramos, G. C., Fernandes, D., Charao, C. T., Souza, D. G., Teixeira, M. M., & Assreuy, J. (2007, Jul). Apoptotic mimicry: phosphatidylserine liposomes reduce inflammation through activation of peroxisome proliferator-activated receptors (PPARs) in vivo. *British Journal of Pharmacology*, *151*(6), 844-850.
- Ren, Y., Xie, Y., Jiang, G., Fan, J., Yeung, J., Li, W., Tam, P. K., & Savill, J. (2008, Apr 1). Apoptotic cells protect mice against lipopolysaccharide-induced shock. *J Immunol*, *180*(7), 4978-4985.
- Sevilla, P., Cirera, A., Dotor, J., Gil, F. J., Galindo-Moreno, P., & Aparicio, C. (2018, May 23). In vitro cell response on CP-Ti surfaces functionalized with TGF- β 1 inhibitory peptides. *J Mater Sci Mater Med*, *29*(6), 73.
- Sheikh, Z., Brooks, P. J., Barzilay, O., Fine, N., & Glogauer, M. (2015, Sep). Macrophages, Foreign Body Giant Cells and Their Response to Implantable Biomaterials. *Materials*, *8*(9), 5671-5701.
- Shull, M. M., Ormsby, I., Kiert, A. B., Pawlowski, S., Diebold, R. J., Yin, M., Allen, R., Sidman, C., Proetzel, G., Calvint, D., Annunziatata, N., & Doetschman, T. (1992). Targeted disruption of the mouse transforming growth factor- β 1 gene results in multifocal inflammatory disease. *Nature*, *359*(6397), 693-699.

- Wang, J., Qian, S., Liu, X., Xu, L., Miao, X., Xu, Z., Cao, L., Wang, H., & Jiang, X. (2017A, May 14). M2 macrophages contribute to osteogenesis and angiogenesis on nanotubular TiO₂ surfaces. *Journal of Materials Chemistry B*, *5*(18), 3364–3376.
- Wang, L., Yang, J., Ran, B., Yang, X., Zheng, W., Long, Y., & Jiang, X. (2017B, Sep 27). Small Molecular TGF- β 1-Inhibitor-Loaded Electrospun Fibrous Scaffolds for Preventing Hypertrophic Scars. *ACS Appl Mater Interfaces*, *9*(38), 32545–32553.
- Watanabe, S., Alexander, M., Misharin, A. V., & Budinger, G. R. S. (2019, May 20). The role of macrophages in the resolution of inflammation. *J Clin Invest*, *129*(7), 2619–2628.
- Wynn, T. A., & Vannella, K. M. (2016, Mar 15). Macrophages in Tissue Repair, Regeneration, and Fibrosis. *Immunity*, *44*(3), 450–462.
- Yamada, K., Uchiyama, A., Uehara, A., Perera, B., Ogino, S., Yokoyama, Y., Takeuchi, Y., Udey, M. C., Ishikawa, O., & Motegi, S. (2016, Jul 15). MFG-E8 Drives Melanoma Growth by Stimulating Mesenchymal Stromal Cell-Induced Angiogenesis and M2 Polarization of Tumor-Associated Macrophages. *Cancer Res*, *76*(14), 4283–4292.
- Zhang, F., Wang, H., Wang, X., Jiang, G., Liu, H., Zhang, G., Wang, H., Fang, R., Bu, X., Cai, S., & Du, J. (2016, Aug 9). TGF- β induces M2-like macrophage polarization via SNAIL-mediated suppression of a pro-inflammatory phenotype. *Oncotarget*, *7*(32), 52294–52306.
- Ziegler-Heitbrock, L., Ancuta, P., Crowe, S., Dalod, M., Grau, V., Hart, D. N., Leenen, P. J., Liu, Y. J., MacPherson, G., Randolph, G. J., Scherberich, J., Schmitz, J., Shortman, K., Sozzani, S., Strobl, H., Zembala, M., Austyn, J. M., & Lutz, M. B. (2010, Oct 21). Nomenclature of monocytes and dendritic cells in blood. *Blood*, *116*(16), e74–80.

Abstract in Korean

대식세포는 이물질에 대한 염증 반응에 있어서 중요한 역할을 한다. 상처 치유와 골 형성에 있어 M1/M2형 대식세포가 분비하는 사이토카인은 다르게 작용한다. 과거 연구에서는 사멸 세포를 모방한 포스파티딜세린 리포솜 (PSLs)을 이용하여 대식세포의 항염증 반응을 증폭시켰다. 본 연구의 목적은 이 PSLs의 표면을 개질하여 이물질에 대한 염증반응에서 대식세포의 분극을 조절하고자 하였다.

먼저 PSLs의 표면을 arginine-glycine-aspartate (RGD)로 개질하였다. RGD는 milk fat globule-epidermal growth factor-factor 8 (MFG-E8)의 RGD-motif를 모방한다. 이는 대식세포의 $\alpha v\beta 3/\alpha v\beta 5$ -integrins에 결합하여 대식세포의 식세포작용을 통해 항염증반응을 유도한다. In vitro 실험의 결과에서는 bone marrow derived macrophage의 arg-1, FIZZ1 그리고 YM-1의 mRNA 발현이 3 % RGD-PSLs에서 0 % RGD-PSLs 대비 상승한 것을 확인하였고, arg-1와 CCL17의 단백질 또한 통계학적 유의하게 3 % RGD-PSLs에서 상승하였다. 또한 LPS로 유도된 M1 대식세포가 3 % RGD-PSLs에 의해 억제되었는데, IL-1 β , IL-6와 TNF- α 의 mRNA 발현이 0 %와 1 % RGD-PSLs 대비 감소되었다. 이와 같은 결과는 iNOS와 TNF- α ELISA에서도 확인하였다. FACs와 면역 형광 분석에서 3 % RGD-PSLs가 대식세포의 M2형 분극을 촉진하였고, LPS로 유도된 M1 대식세포 억제하는 것을 확인할 수 있었다. N-(6-tetramethyl-rhodaminethiocarbonyl)-1,2-dihexadecanoyl-sn-glycero-3-phosphatidyl ethanol-amine (TRITC-DHPE)로 라벨 된 리포솜을 BMDM에 처리한 결과에서는 3 % RGD-PSLs가 가장 높은 흡수를 보였다.

In vivo에서는 RGD-PSLs가 포함된 알지네이트-젤라틴 PVA를 Sprague Dawley (SD) 랫드에 피하주사 하였다. 1 주 뒤 PVA 스캐폴드에 조직재생을 측정하였고, 대식세포의 분극을 면역조직학적 염색으로

분석하였다. 4 주 뒤에는 Masson's trichrome 염색을 통해 PVA 주위에 형성된 조직 섬유를 측정하였다. 결과로는 1 주 뒤 카라지난으로 유도된 M1 대식세포가 0 %와 3 % RGD-PSLs에서 억제된 것을 확인하였다. 하지만 M2 대식세포에서는 실험군 간 차이를 보이지 않았다. 또한 1 주 뒤 3 % RGD-PSLs에서 가장 높은 조직 재생을 보였고, 4 주 뒤에는 가장 억제된 조직 섬유화를 보였다.

따라서 3 % RGD-PSLs가 리포솜의 식세포작용을 향상시켜 대식세포의 M2형 분극을 촉진하였다고 추측할 수 있다. 또한 조직 섬유화에 있어서는 대식세포의 염증축진이 항염증 반응보다 더 관여하는 것을 확인하였다.

또 다른 PSLs의 표면 개질로는 polyethylene-glycol (PEG)를 사용하였다. PEG로 개질된 PSLs (PEG-PSLs)는 IL-4로 유도된 RAW 264.7 세포의 TGF- β 분비와 multinucleated giant cell (MGC)의 형성을 억제하였다. 하지만 PSLs는 또한 MGC의 형성을 억제시키는 반면, TGF- β 의 분비 조절에서는 효과를 보이지 못했다. In vivo에서는 PEG-PSLs가 함유된 알지네이트-젤라틴 매트릭스를 mixed cellulose ester (MCE) 멤브레인에 코팅한 뒤 SD 랫드의 등에 피하이식 하였다. 4 주 뒤 MCE 멤브레인 주위에 형성된 조직 섬유화를 분석하였다. 결과로는 PSLs에서는 조직 섬유화 억제에 효과를 안보였고, PEG-PSLs에서 조직 섬유화가 줄어든 것을 확인할 수 있었다. 따라서 TGF- β 가 조직 섬유화에 매개하는 중요한 요소인 것을 확인하였다.

RGD와 PEG로 표면 개질된 PSLs의 in vitro와 in vivo 실험에서 대식세포는 각각 다른 분극 효과를 보여주었다. 3 % RGD-PSLs는 PSLs의 항염증 반응 증폭과 PEG-PSLs의 TGF- β 와 조직 섬유화 억제 효과를 입증하였다. 이러한 효과는 PSLs의 표면 개질을 통해 대식세포 분극을 조절하고 이를 통해 상처 치유와 골 재생을 위한 임상에서의 활용 가능성을 보여준다.

주요어 : 대식세포, 분극, 포스파티딜세린, 리포솜, 아르기닌-글리신-아스파르트 , 폴리에틸렌글리콜

학번 : 2016-39051